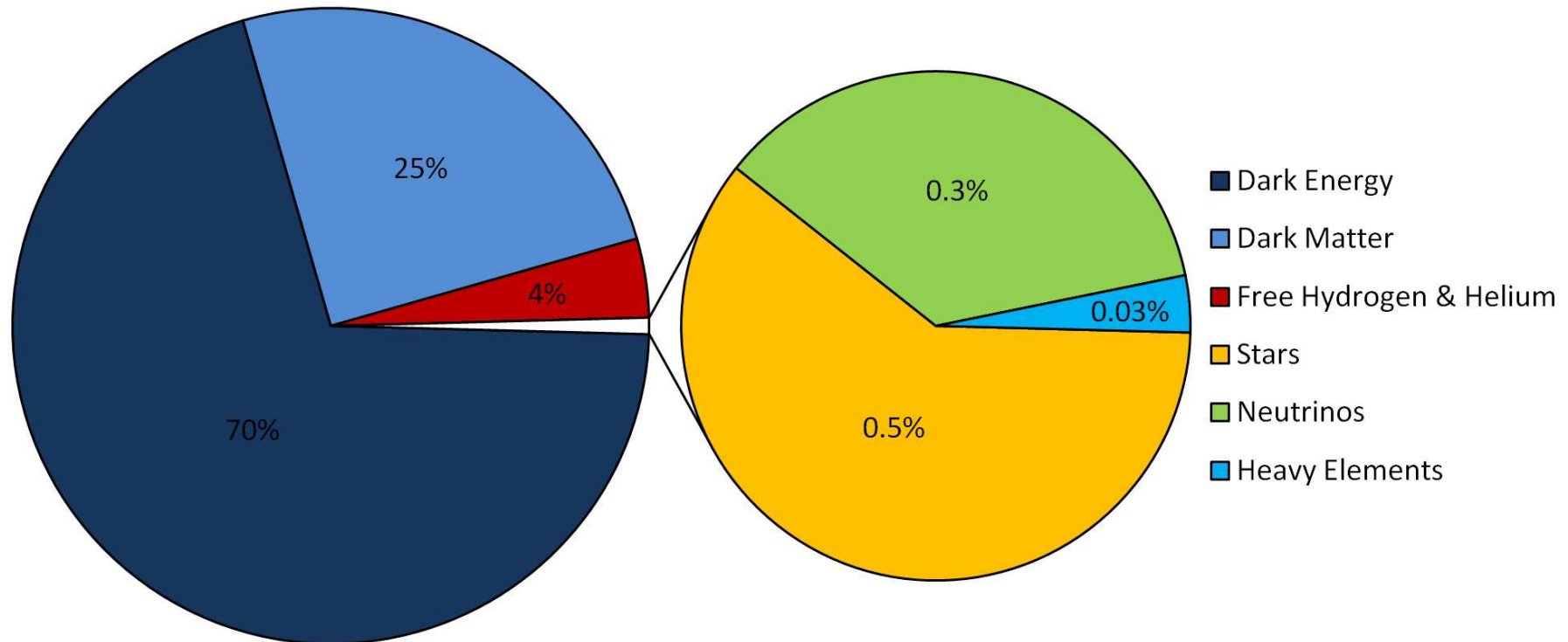

Direct detection of WIMP Dark Matter

Pijushpani Bhattacharjee

`pijush.bhattacharjee@saha.ac.in`

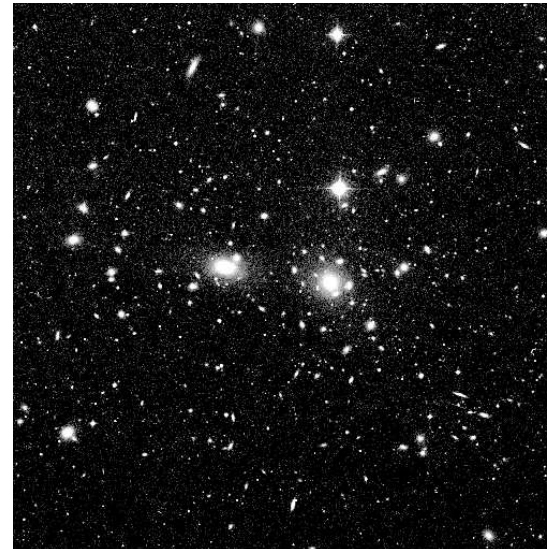
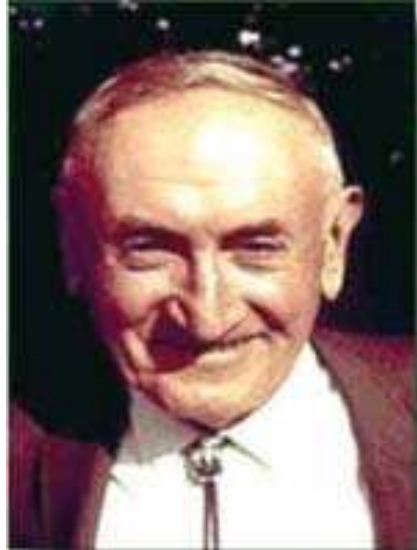
*AstroParticle Physics & Cosmology Division
and Center for Astroparticle Physics,
Saha Institute of Nuclear Physics, Kolkata*

Contents of the Universe



Dark Matter

“Discovered” by Fritz Zwicky in 1933 : “Virial discrepancy” in the Coma cluster :



Coma Cluster

$$\text{Virial Theorem} \Rightarrow \langle v^2 \rangle \sim \frac{1}{2} \frac{GM}{\langle r \rangle}$$

$$\text{Measured } \langle v^2 \rangle^{\frac{1}{2}} \sim 1000 \text{ km s}^{-1} \Rightarrow \langle \rho_{\text{Coma}}^{\text{vir}} \rangle \sim 400 \langle \rho_{\text{visible}} \rangle !!$$

— Radial velocities of galaxies in the Coma cluster are too large to be bound in the cluster with the known “visible” mass of the cluster.

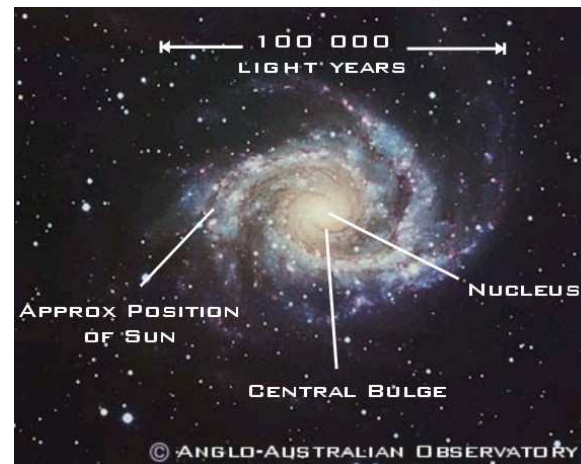
Note: Zwicky used (wrong!) $H_0 = 558 \text{ km s}^{-1} \text{ Mpc}^{-1}$ (as measured by Hubble!).

With $H_0 = 70 \text{ km s}^{-1} \text{ Mpc}^{-1}$, we get $\langle \rho_{\text{Coma}}^{\text{vir}} \rangle \sim 50 \langle \rho_{\text{visible}} \rangle$

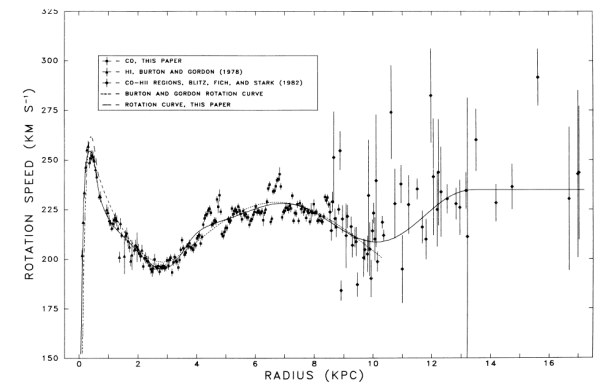
Rotation Curve of Spiral Galaxies and Dark Matter

Galactic scale Dark Matter seriously studied only begining early 1970s: **Vera Rubin:** Rotation Curve of Spiral galaxies. Circular Rotation Speed: $v_c^2(R) = R \frac{\partial \phi}{\partial R} = G \frac{M(R)}{R}$

Rotation Curve of Milky Way



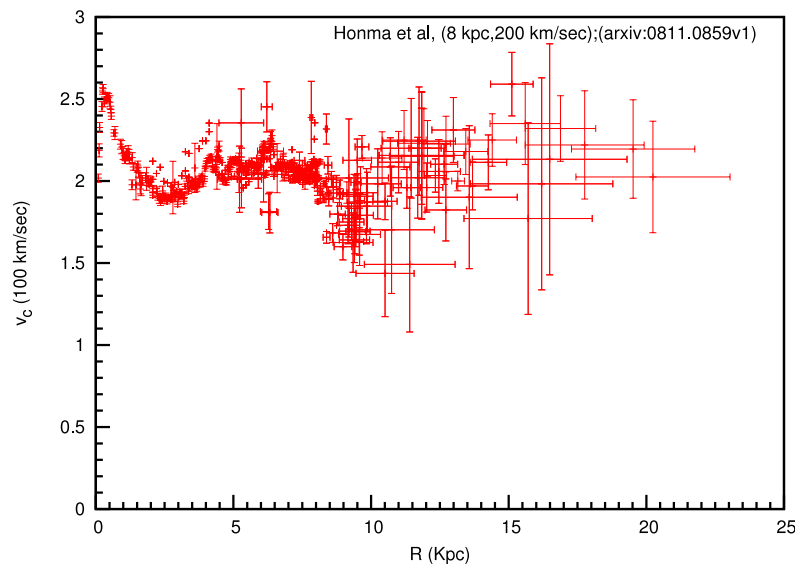
Milky Way



Clemens (1985)

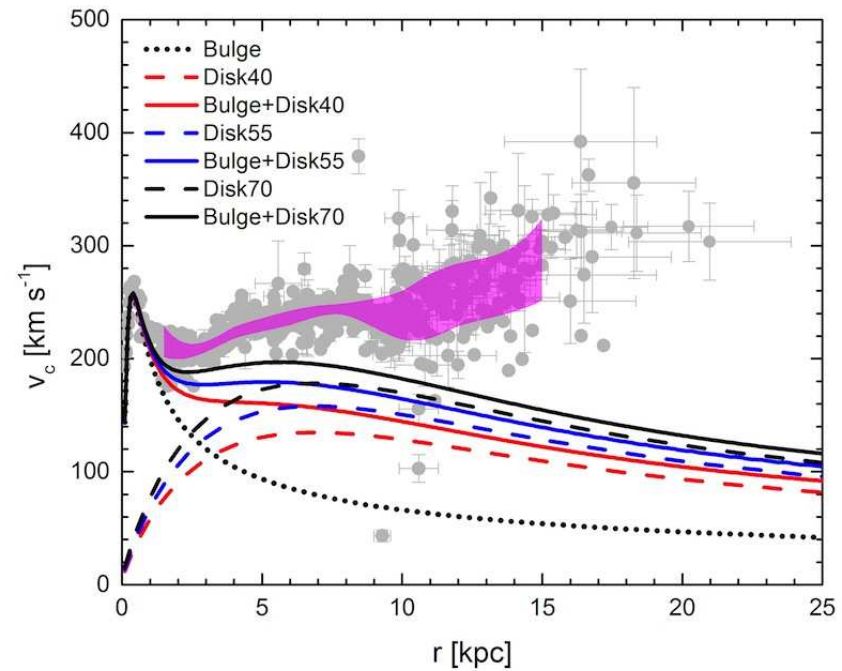
Vera Rubin

Milky Way's Rotation Curve (to ~ 20 kpc)



$$R_0 = 8 \text{ kpc}, V_0 = 200 \text{ km s}^{-1}$$

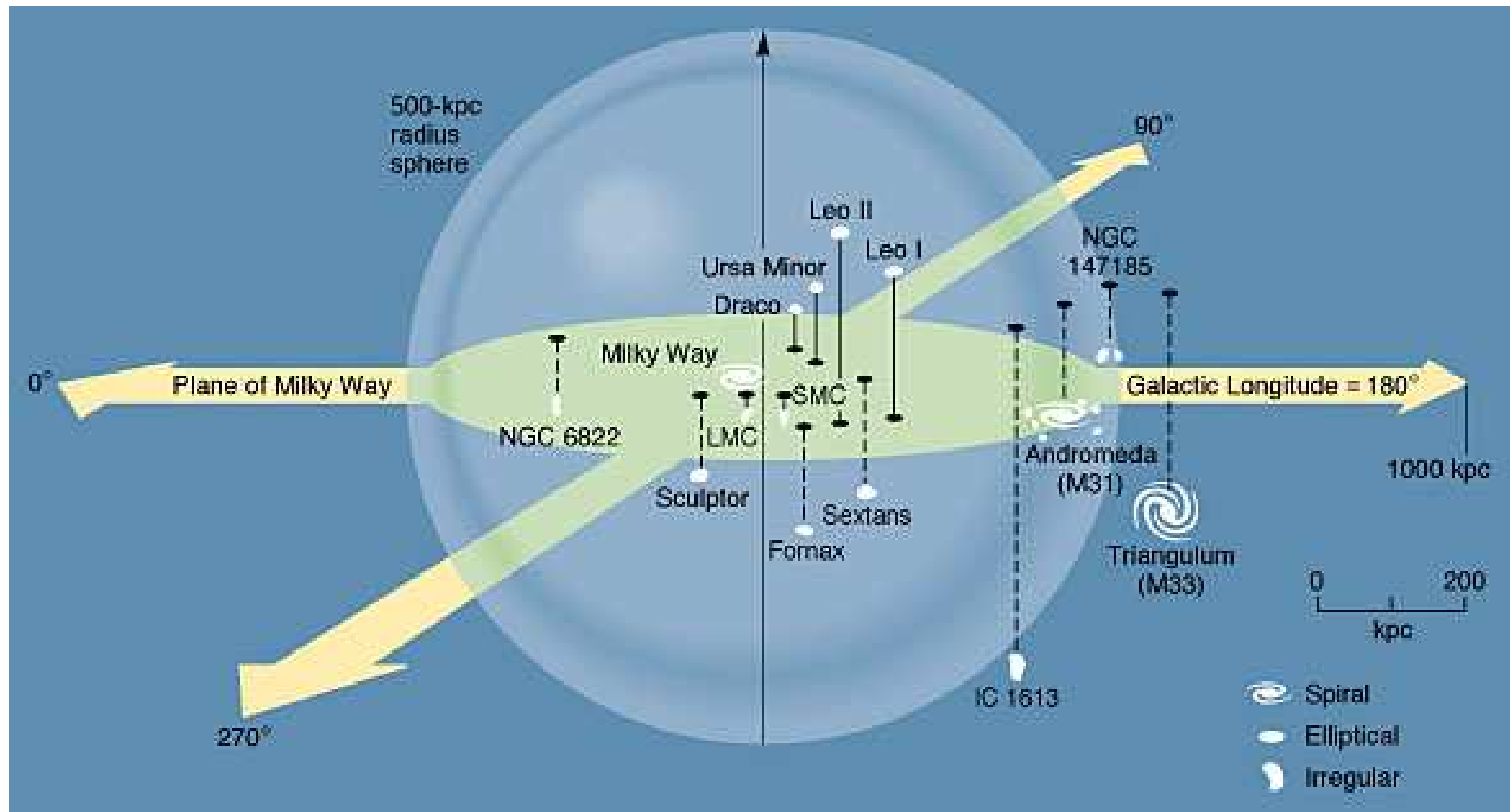
Honma et al, arXiv:0811.0859



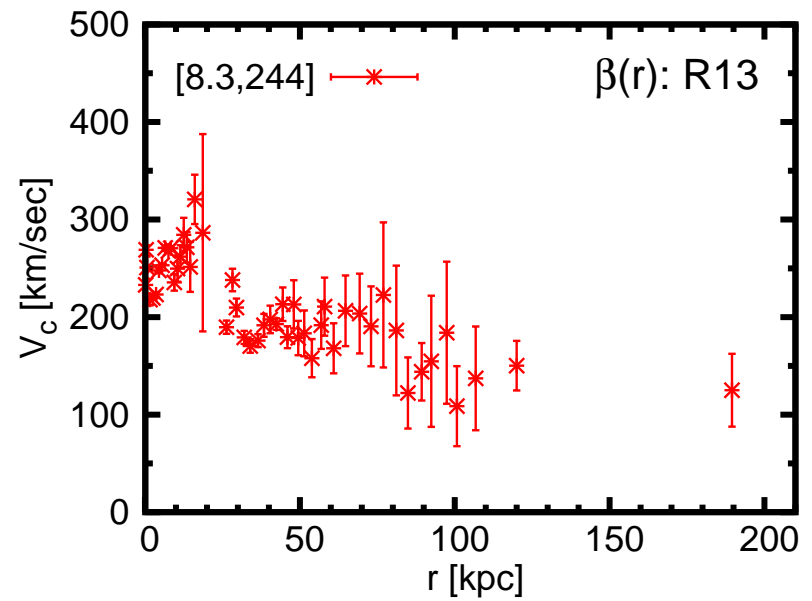
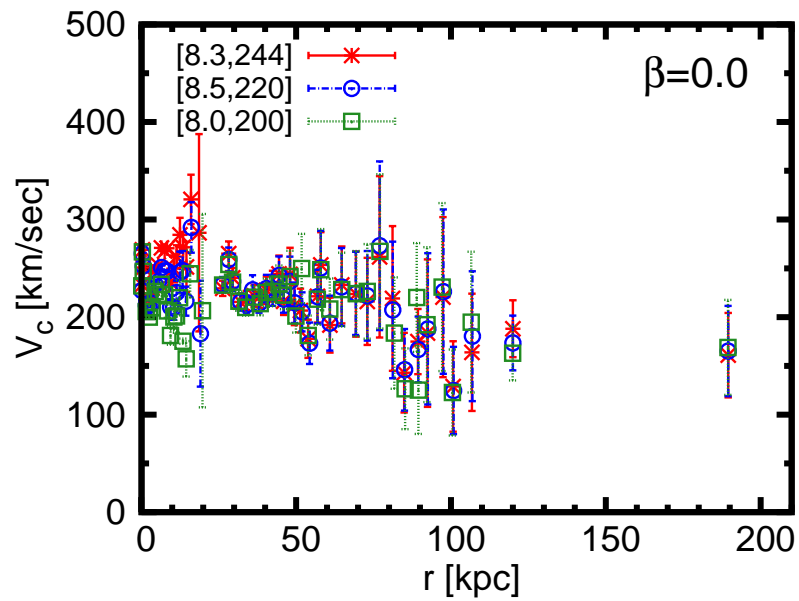
$$R_0 = 8.3 \text{ kpc}, V_0 = 240 \text{ km s}^{-1}$$

Burch & Cowsik, ApJ (2013) [arXiv:1306.1920]

The local group

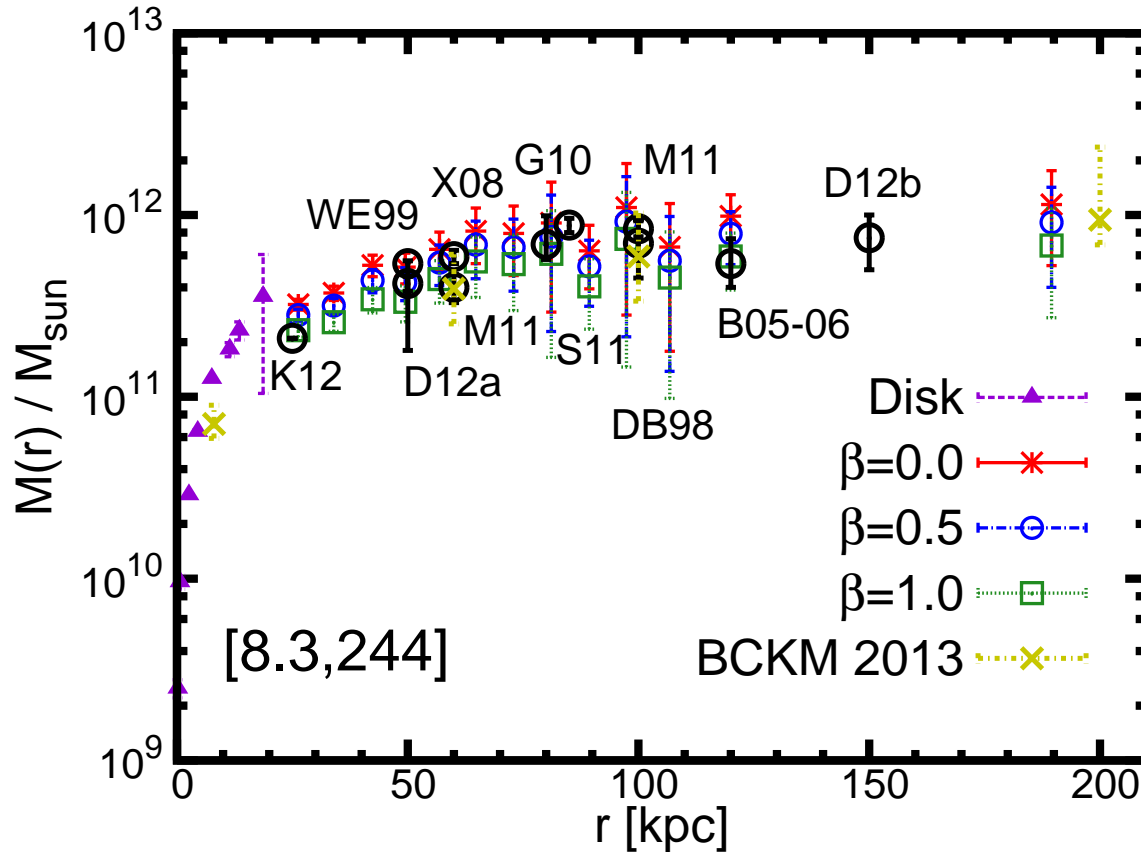


Milky Way's Rotation Curve (to ~ 200 kpc)



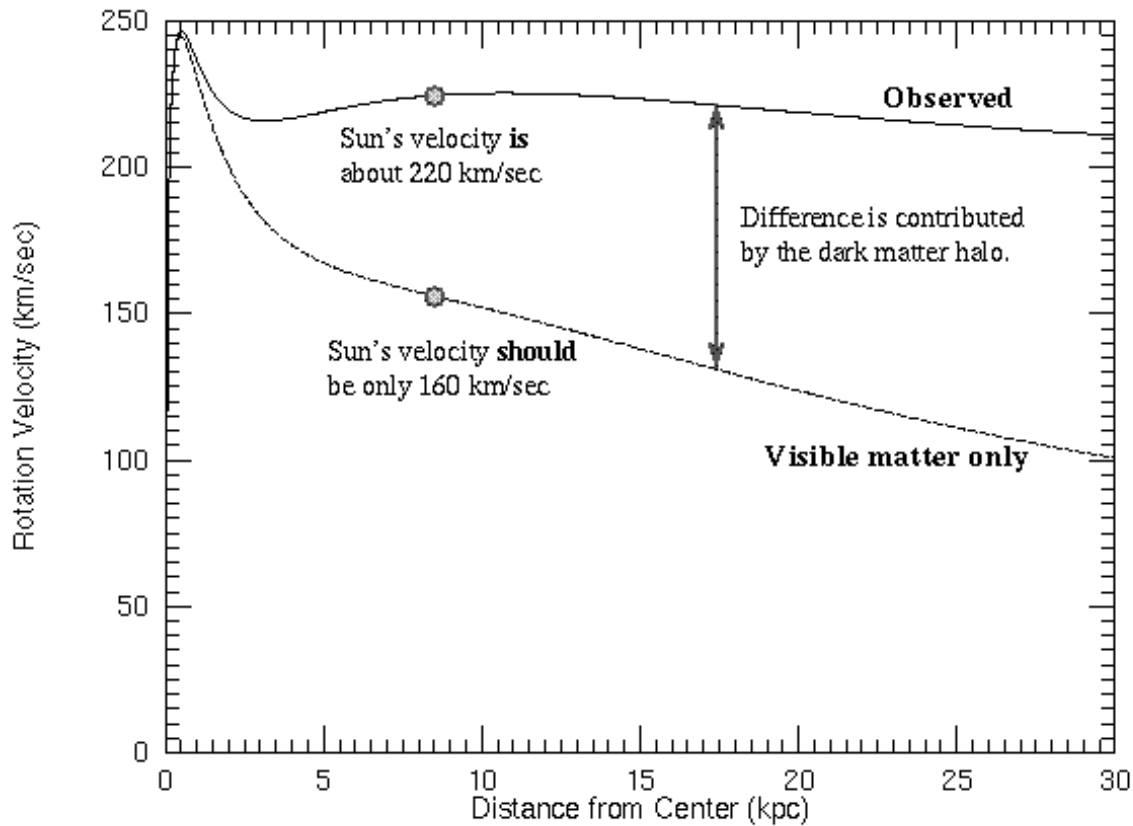
PB, S. Chaudhury & S. Kundu, ApJ (2014) [arXiv:1310.2659]

Mass of the Galaxy

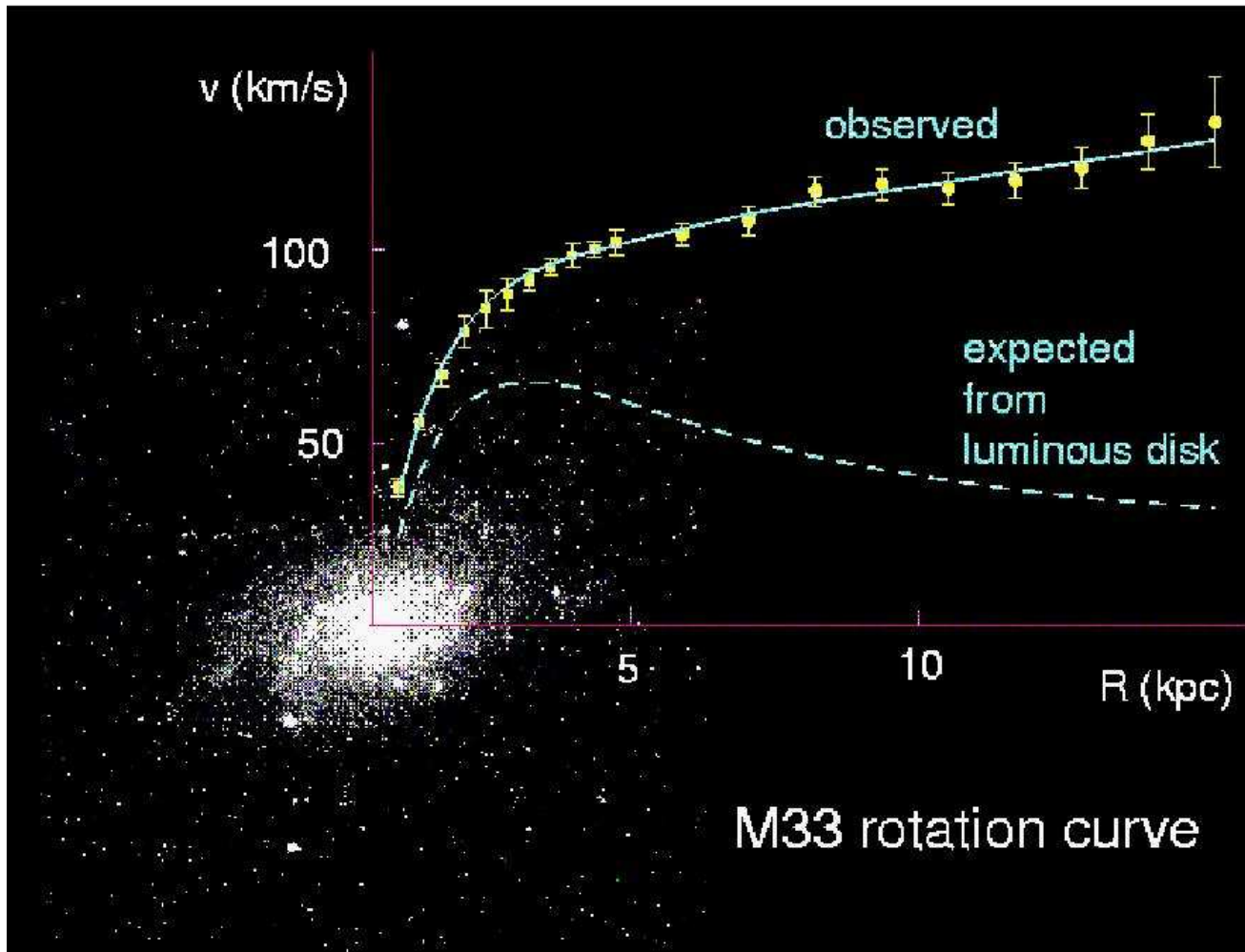


$$M(200 \text{ kpc}) \gtrsim (6.8 \pm 4.1) \times 10^{11} M_{\odot}, \text{ (with } \beta = 1)$$

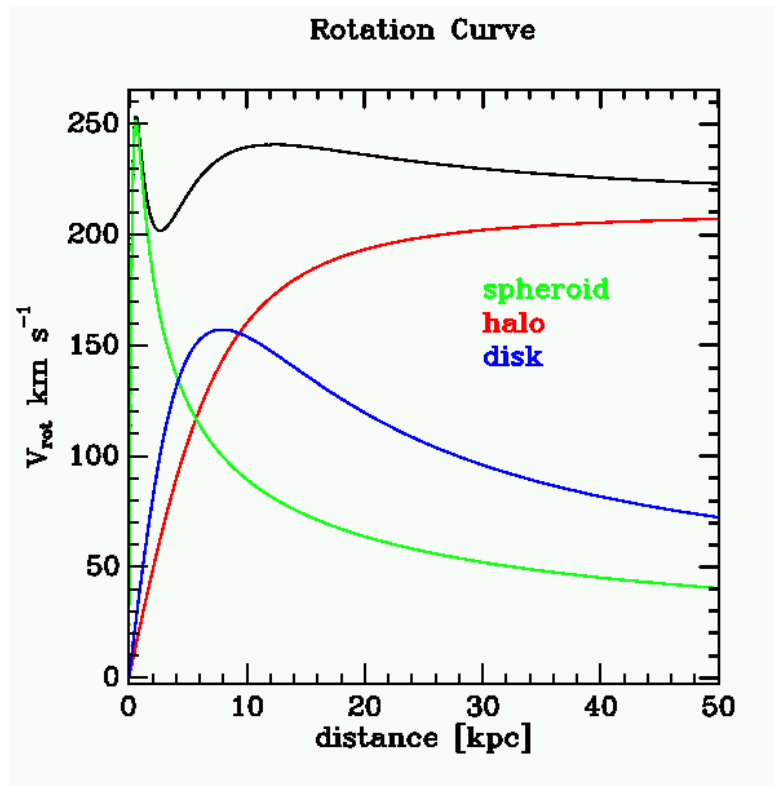
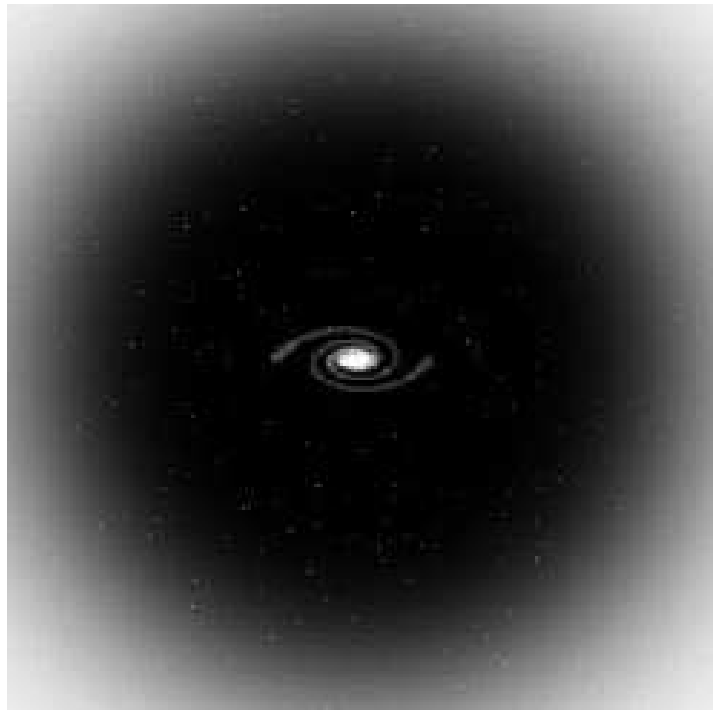
PB, S. Chaudhury & S. Kundu, ApJ (2014) [arXiv:1310.2659]



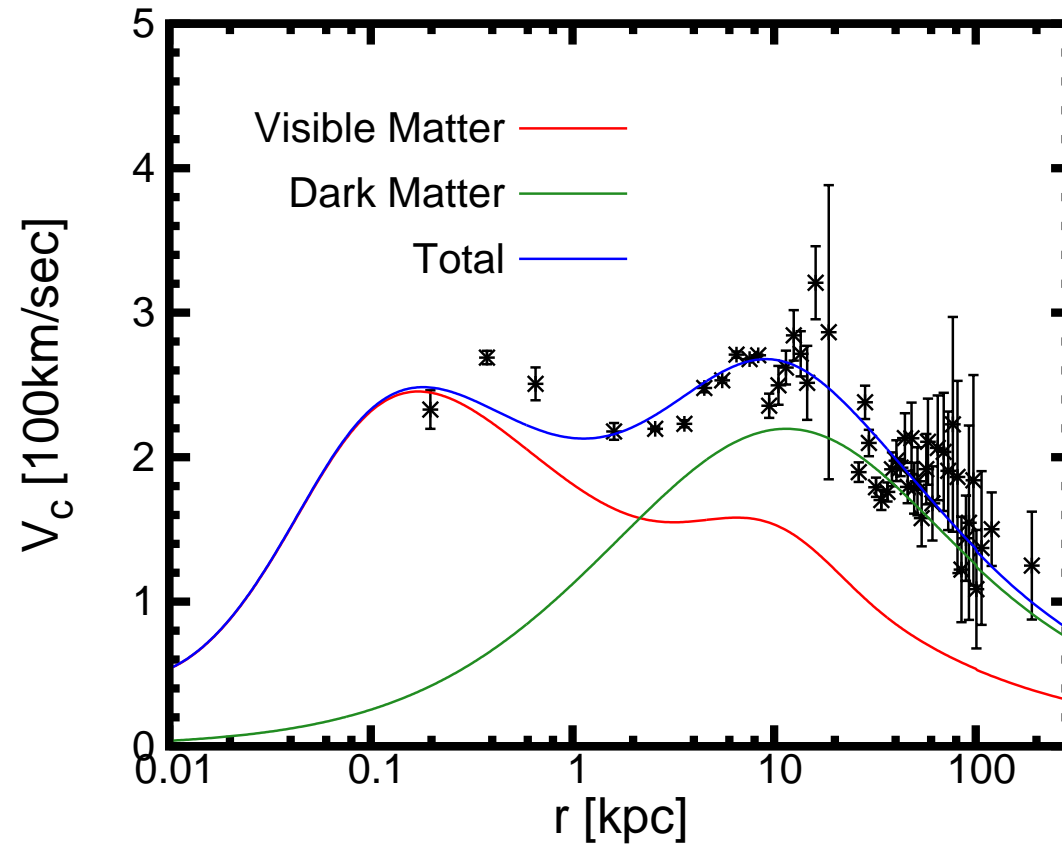
The gravity of the visible matter in the Galaxy is not enough to explain the high orbital speeds of stars in the Galaxy. For example, the Sun is moving about 60 km/sec too fast. The part of the rotation curve contributed by the visible matter only is the bottom curve. The discrepancy between the two curves is evidence for a **dark matter halo**.



Mass Models : Dark Matter Halo

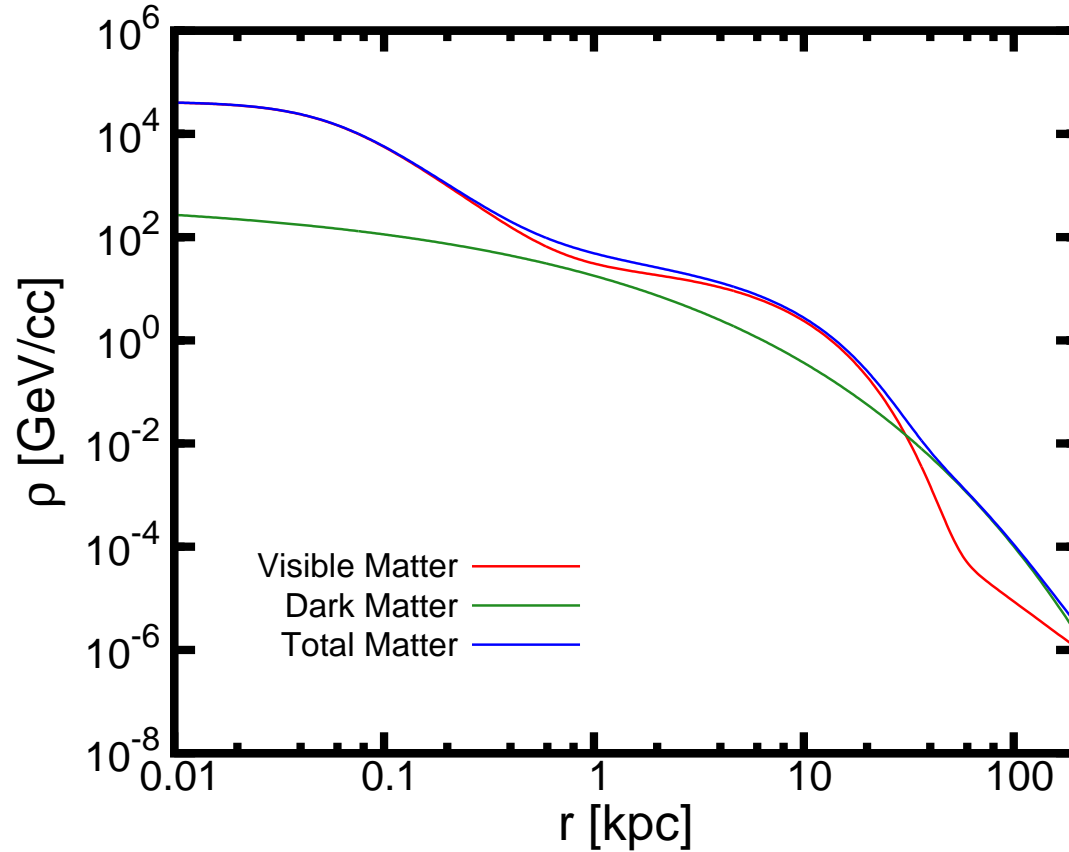


Rotation Curve fit with Einasto density profile of DM



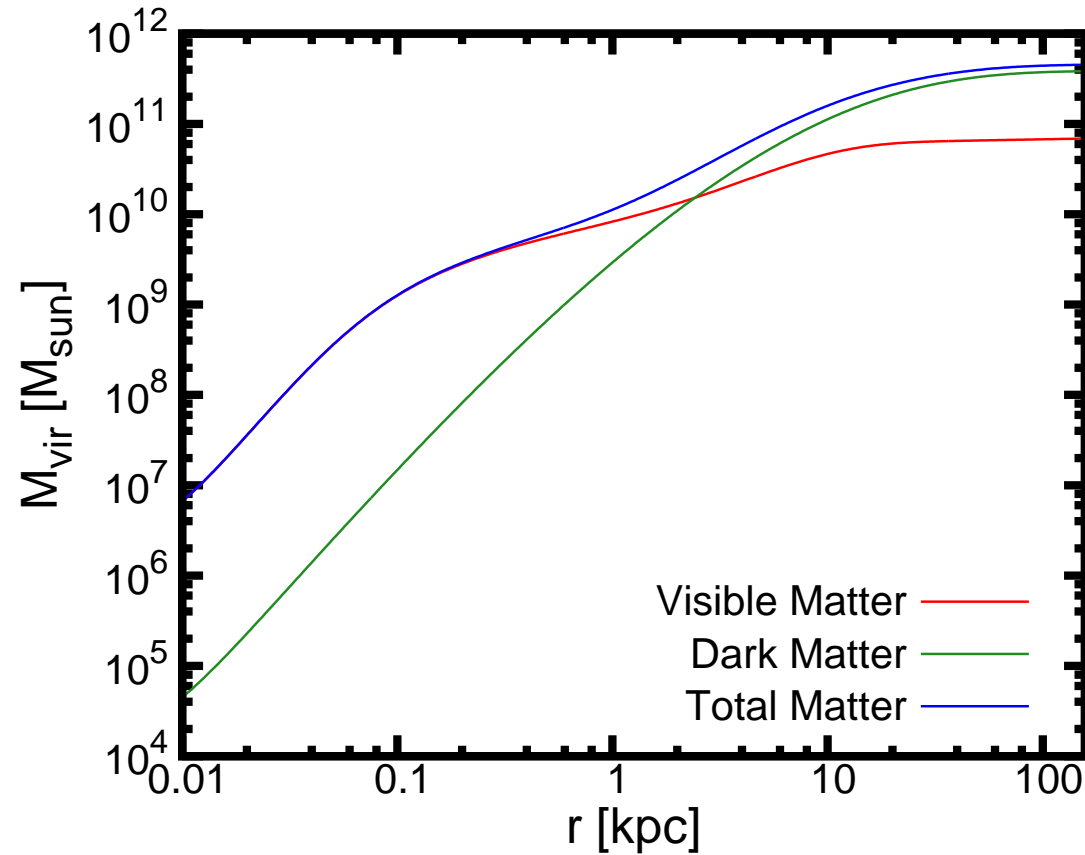
PB, S. Chaudhury & S. Kundu (2014)

Rotation Curve fit with Einasto density profile of DM



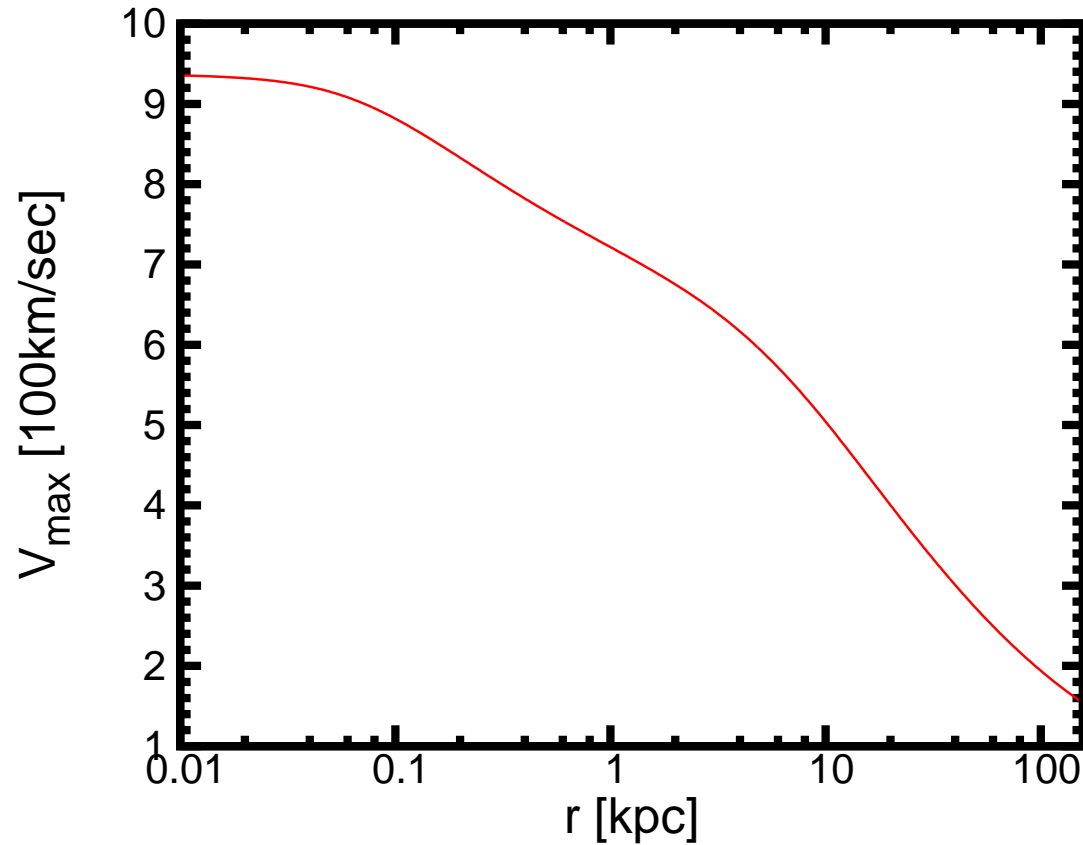
PB, S. Chaudhury & S. Kundu (2014)

Rotation Curve fit with Einasto density profile of DM



PB, S. Chaudhury & S. Kundu (2014)

Rotation Curve fit with Einasto density profile of DM



PB, S. Chaudhury & S. Kundu (2014)

The Nature of Dark Matter

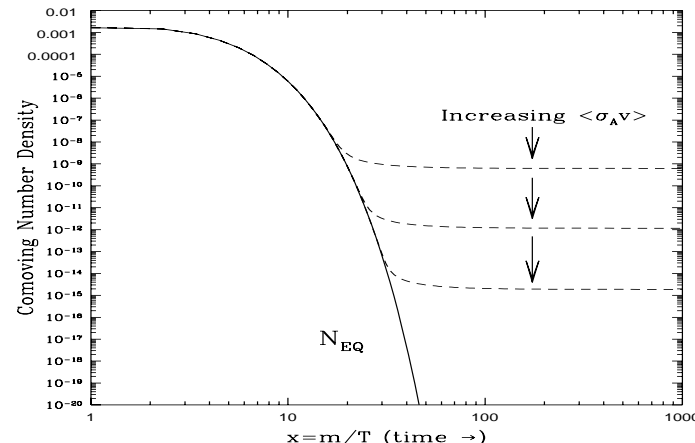


“Bullet Cluster”

- In thermal equilibrium,
 $(n/s)^{\text{eq}} \propto (m/T)^{3/2} e^{-m/T} \Rightarrow$
negligible abundance today!

- But WIMPs can decouple (“freeze out”) when
 $\Gamma_{\text{int}} < H$ in the early universe and survive
with $\Omega_{\text{WIMP}} \propto \langle \sigma_{\text{ann}} v \rangle^{-1}$ today.

- DM must be non-baryonic,
dissipationless \Rightarrow collisionless
 \Rightarrow very weakly interacting
- Clustered on small (sub-galactic)
scale \Rightarrow Must be cold
 \Rightarrow Weakly Interacting (Massive?)
Particles



WIMP abundance today:

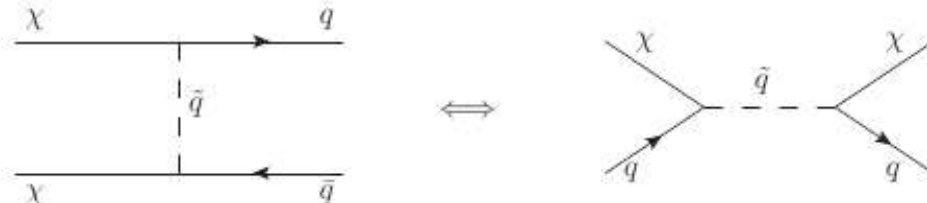
$$\Omega_\chi h^2 \sim 0.1 \left(\frac{3 \times 10^{-26} \text{ cm}^3 / \text{sec}}{\langle \sigma v \rangle} \right) + \log \text{ corrections}$$

Typically, $\sigma \sim \alpha^2 / m_\chi \sim 10^{-8} \text{ GeV}^{-2} \sim 4 \times 10^{-36} \text{ cm}^2$ (with $\alpha \sim 10^{-2}$ $m_\chi \sim 100 \text{ GeV}$), and $\langle v \rangle_f \sim 0.25c$. Also, $h \sim 0.7$.

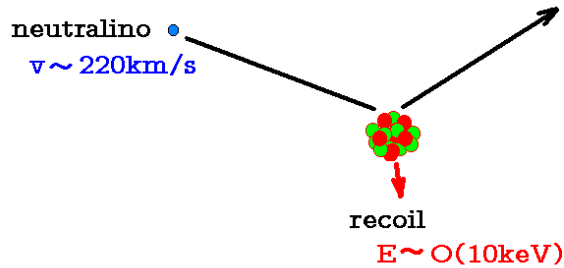
Thus, if there is a WIMP, it is a natural DM candidate!

WIMP annihilation into SM particles \Rightarrow WIMPs must also have some (weak) interaction (albeit small) with nuclei, via crossing symmetry \Rightarrow Direct detection of WIMPs may be possible.

Also, WIMPs captured within astrophysical bodies would annihilate \Rightarrow annihilation products (e.g., γ -rays, ν 's) may be detectable. \Rightarrow indirect detection through ν 's from the Sun, γ -rays from Galactic Centre, dwarf Spheroidal galaxies, . . .



Direct Detection: Order-of-magnitude Estimates



Event rate :

For a single detector nucleus, the rate of WIMP scatterings, $R \sim n_\chi v \sigma_{\chi N}$, gives

$$R \sim 2.7 \times 10^{-25} \text{ yr}^{-1} \left(\frac{\rho_\chi}{0.3 \text{ GeV cm}^{-3}} \right) \left(\frac{100 \text{ GeV}}{m_\chi} \right) \left(\frac{v}{300 \text{ km s}^{-1}} \right) \left(\frac{\sigma_{\chi N}}{10^{-37} \text{ cm}^2} \right)$$

No. of nuclei of atomic number A in 1 gm is $6 \times 10^{23}/A$. So, total rate

$$R_{\text{total}} \sim 1.6 \text{ events kg}^{-1} \text{ yr}^{-1} \left(\frac{100}{A} \right) \left(\frac{\rho_\chi}{0.3 \text{ GeV cm}^{-3}} \right) \left(\frac{100 \text{ GeV}}{m_\chi} \right) \left(\frac{v}{300 \text{ km s}^{-1}} \right) \left(\frac{\sigma_{\chi N}}{10^{-37} \text{ cm}^2} \right)$$

Recoil Energy :

For a WIMP of mass m_χ and velocity v striking a nucleus of mass M at rest, $\Delta p \sim m_\chi v$. \Rightarrow Recoil energy of nucleus,

$$E_r \sim (\Delta p)^2 / 2M \sim 50 \text{ keV} \left(\frac{m_\chi}{100 \text{ GeV}} \right)^2 \left(\frac{v}{300 \text{ km s}^{-1}} \right)^2 \left(\frac{100 \text{ GeV}}{M} \right).$$

Proper calculations :

Recoil energy: $E = (\mu^2 v^2 / M)(1 - \cos \theta^*)$, where $\mu \equiv m_\chi M / (m_\chi + M)$ = reduced mass, v = WIMP speed relative to the nucleus, and θ^* = scattering angle in the center of mass frame.

Differential recoil rate per unit detector mass (typically measured in units of counts/day/kg/keV) :

$$\frac{dR}{dE} = \frac{\sigma(q)}{2 m_\chi \mu^2} \rho \eta(E, t) \equiv \text{Particle Physics} \otimes \text{Astrophysics},$$

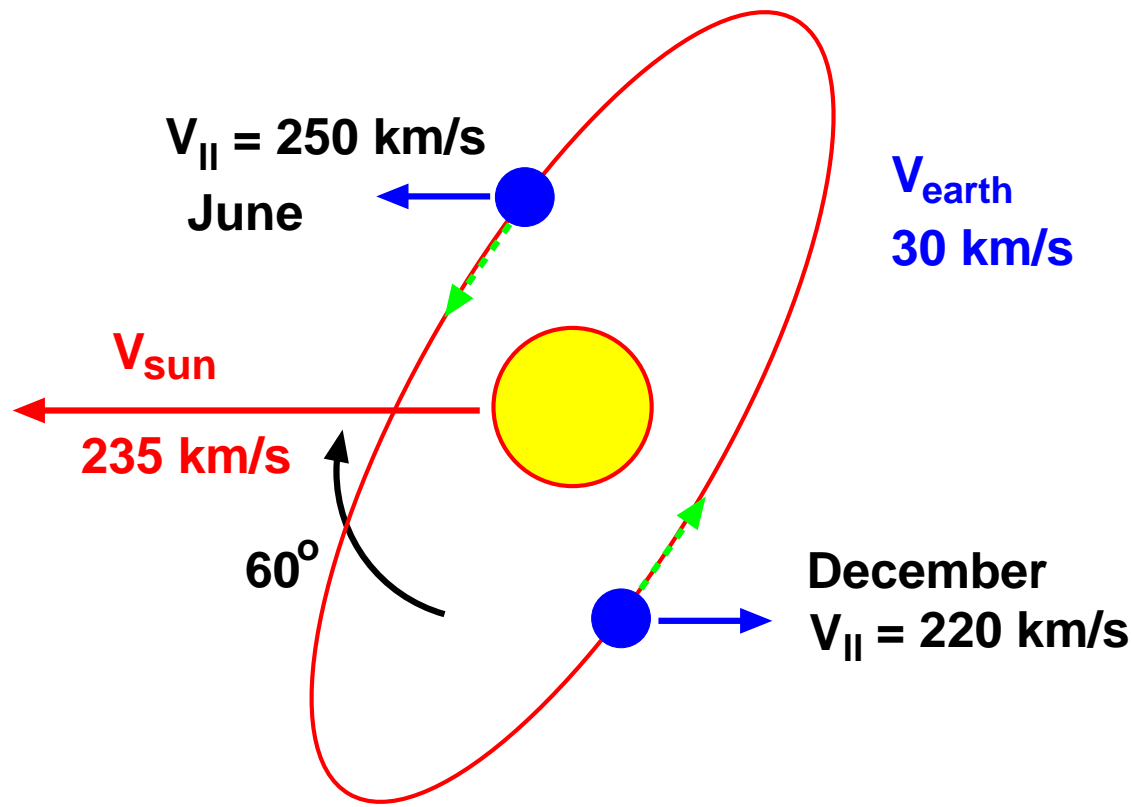
with $q = \sqrt{2ME}$ = nucleus recoil momentum, $\sigma(q)$ = WIMP-nucleus cross-section,

$$\eta(E, t) = \int_{v > v_{\min}} \frac{f(\mathbf{v}, t)}{v} d^3v ,$$

$v_{\min} = \sqrt{\frac{ME}{2\mu^2}}$ = minimum WIMP velocity that can result in a recoil energy E .

$f(\mathbf{v}, t)$ is the (time-dependent) velocity distribution of the WIMPs relative to detector at rest on Earth.

Modulation Signal



$$f(\mathbf{v}, t) = f_{\text{Galaxy}}(\mathbf{v} + \mathbf{v}^{\text{Earth}}(t)).$$

WIMP-Nucleus (Effective) Interactions

The effective WIMP-Nucleus X-section can be obtained from fundamental WIMP-quark/gluon x-section:

$$\sigma_{\chi-A} \leftarrow \sigma_{\chi-N} \leftarrow \sigma_{\chi-q}$$

Spin-independent (SI) interaction:

$$\frac{d\sigma(q)}{dq^2} = \frac{1}{4m_n^2 v^2} \sigma_n A^2 F^2(q)$$

V= WIMP-nucleus relative velocity

WIMP-nucleon x-section

Coherence Form factor:
loss of coherence

WIMP-nucleon reduced mass = nucleon mass for $m_{\text{WIMP}} \gg m_n$

Spin-dependent (SD) Interaction:

$$\frac{d\sigma(q)}{dq^2} = \frac{8}{\pi v^2} \Lambda^2 G_F^2 J(J+1) F^2(q)$$

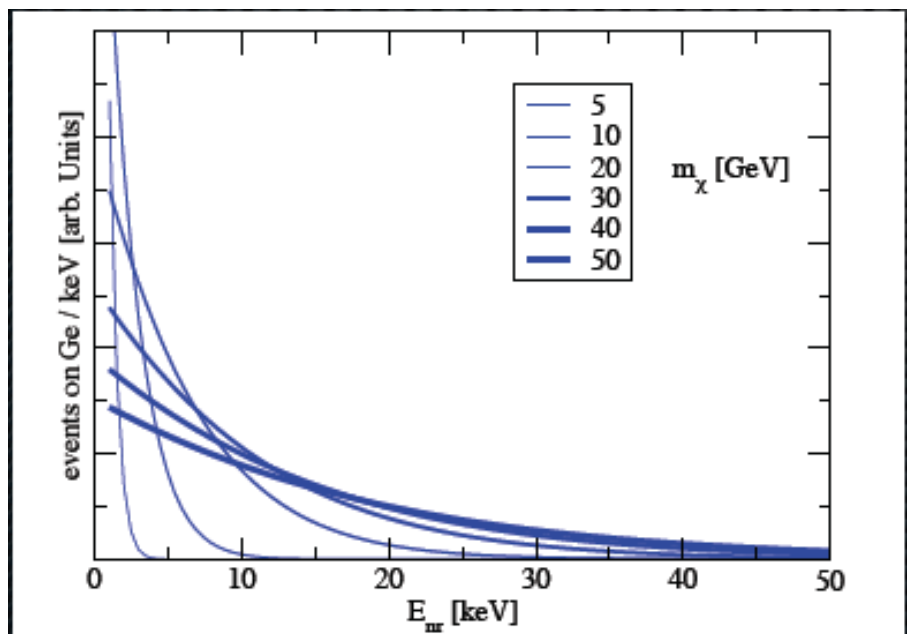
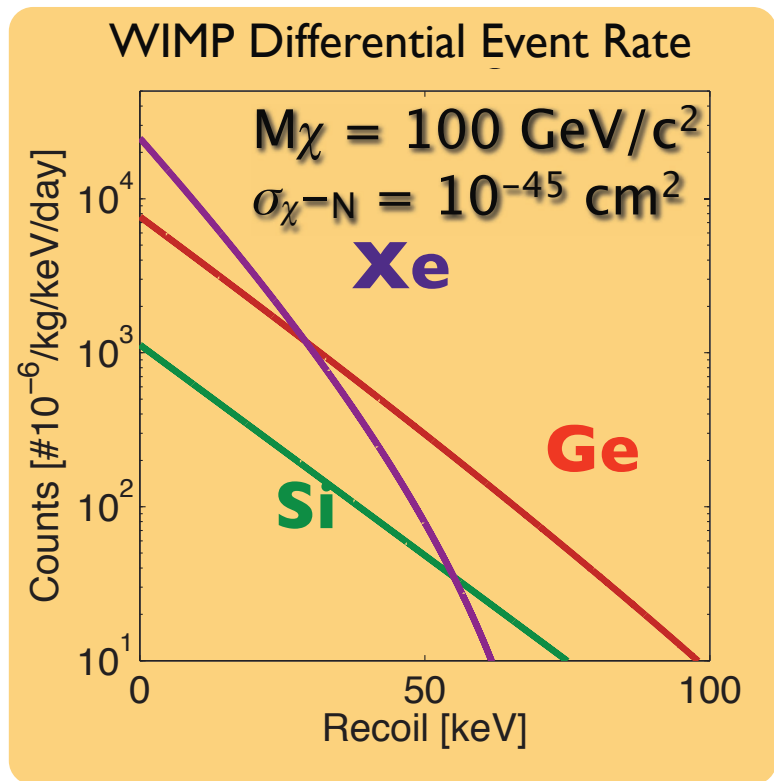
$$\Lambda = \frac{1}{J} \left[a_p \langle S_p \rangle + a_n \langle S_n \rangle \right]$$

$$\langle S_{p,n} \rangle = \langle N | S_{p,n} | N \rangle$$

measure the amount of spin carried by
the p- and n-groups inside the nucleus

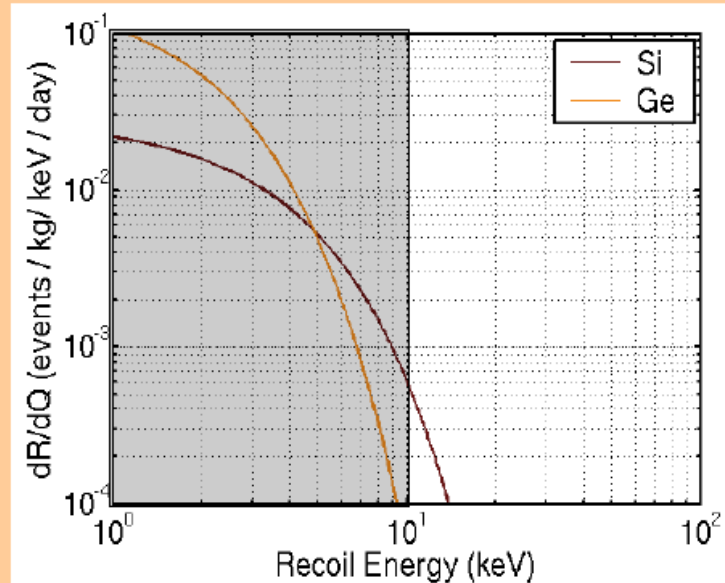
a_p, a_n : effective coupling of the WIMPs to protons and neutrons, typically α/mw^2

Nuclear Recoil Spectrum

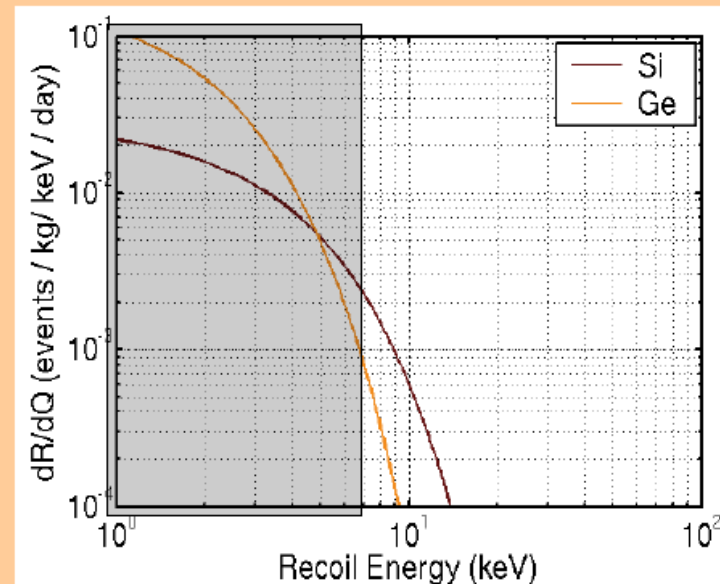


Low mass WIMP: Si vs Ge

$m_{\text{WIMP}} = 8 \text{ GeV}$



$E_{\text{th}} = 10 \text{ keV}$



$E_{\text{th}} = 7 \text{ keV}$

For low mass WIMPs, need lower threshold and lower target nucleus mass

Methods of detecting the nuclear recoil energy

- **Scintillation** : Recoil energy of nucleus taken up by electrons which radiate through scintillation detected by photomultiplier tubes..some part is lost as phonons.

[DAMA,XENON]

Quenching: $E_{obs} = q \times E_r$

For some energies and incident angles:

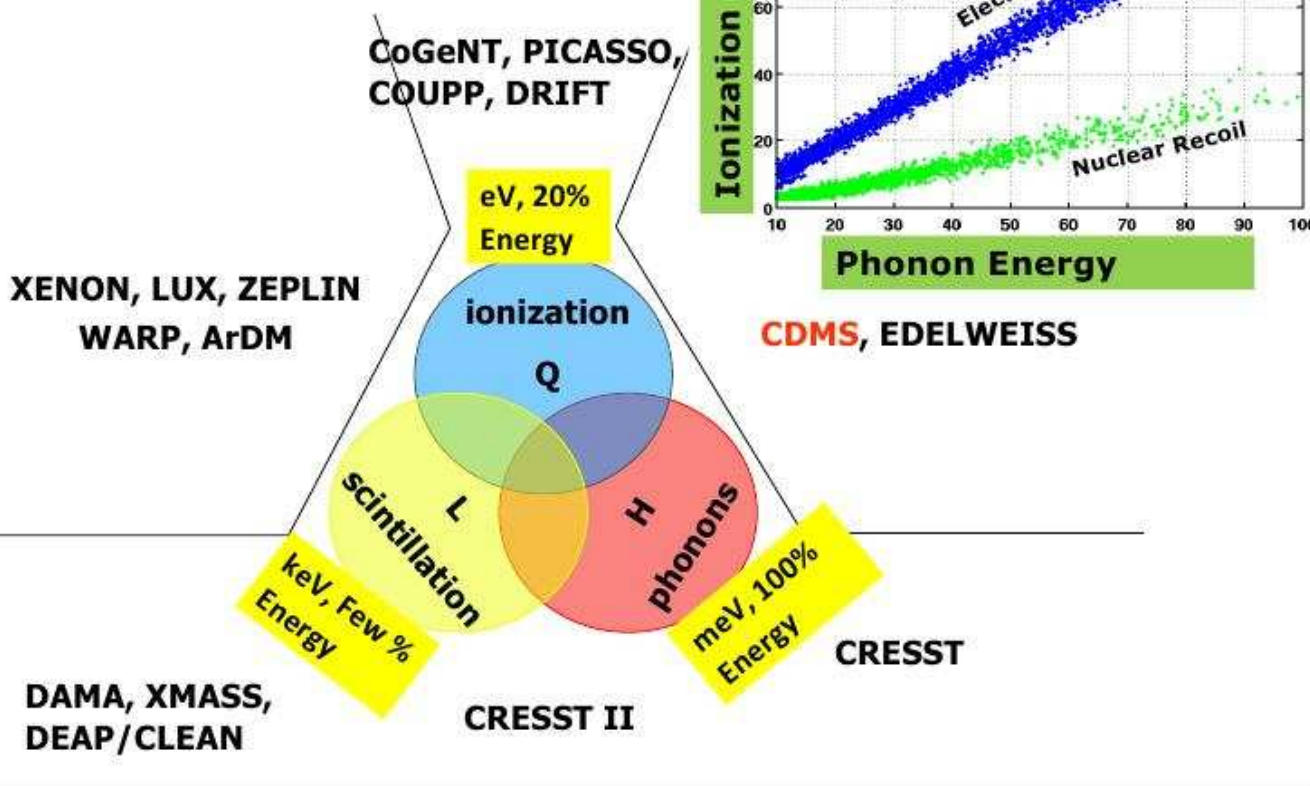
$q=1$: Channeling [Drovyshevski,arxiv:0706.3095]

- **Ionization** : As the nucleus moves through the target mass it ionizes other target atoms and Electrostatic field detected.[CDMS,XENON]

- **Phonons** : Detected by semiconductor and superconductor-junction sensors.

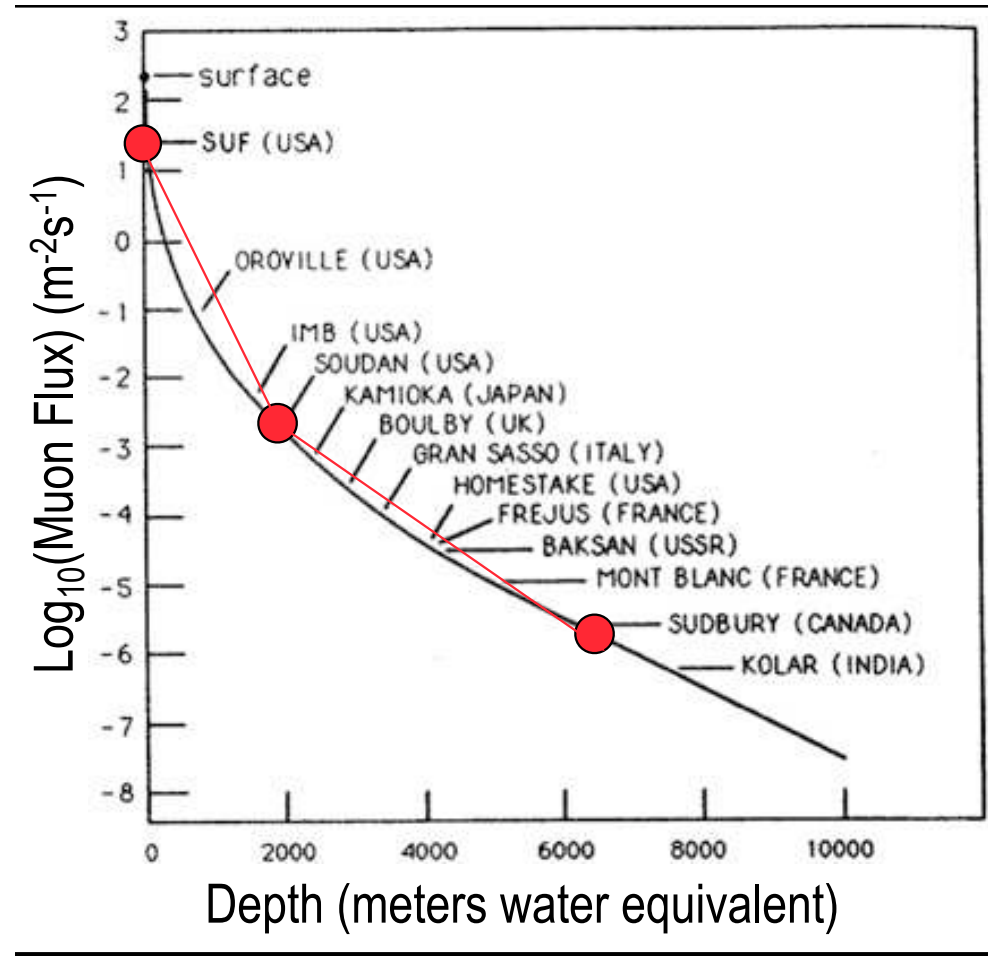
- **Heat** : Recoil energy is detected by change of semiconductor (doped Ge) resistance in a bolometer under cryogenic condition (<50 mK).[CDMS,CRESST]

Detection and Discrimination Methods

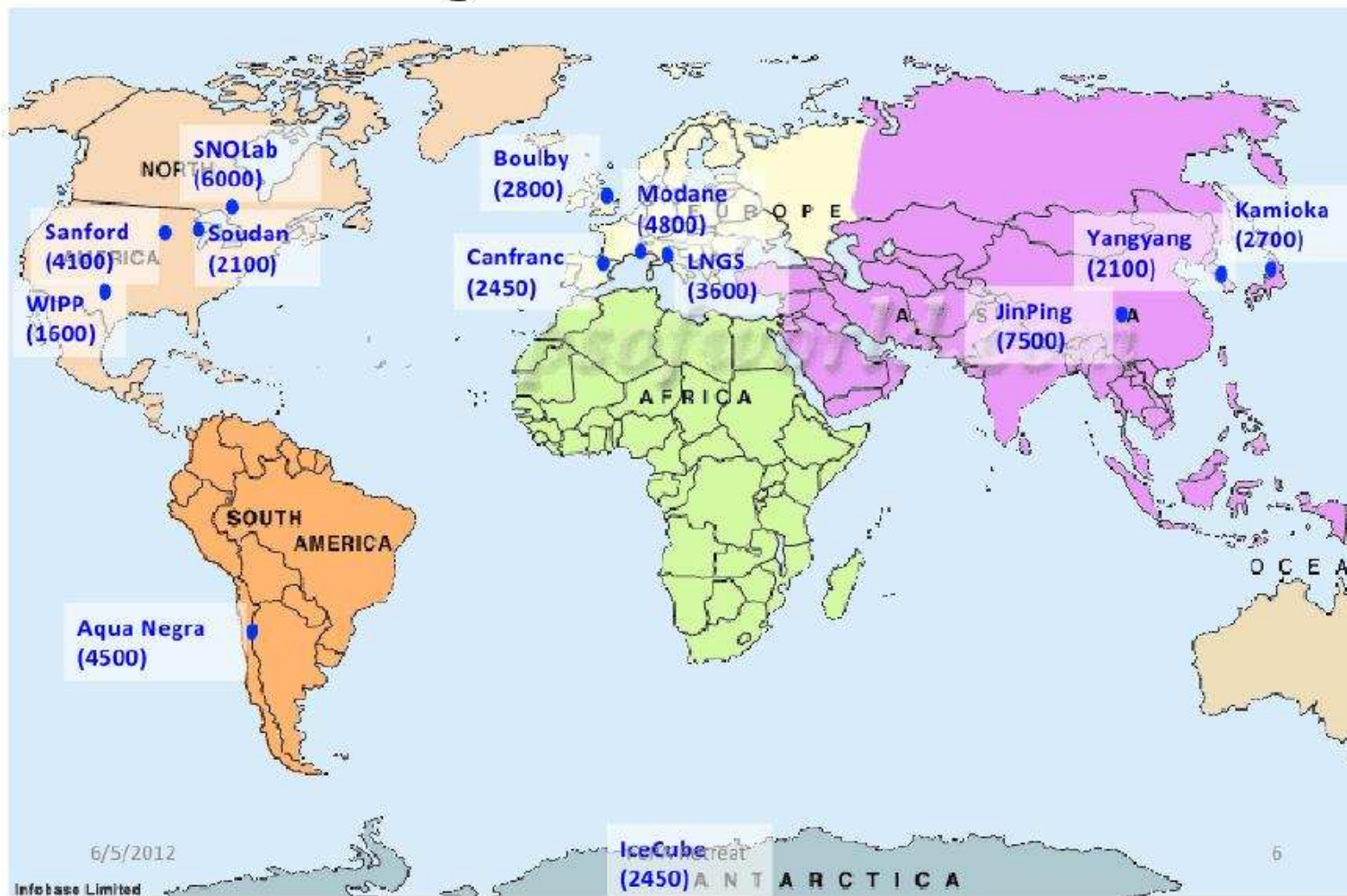


(Source: CDMS)

Go underground to reduce the background :



Underground Laboratories



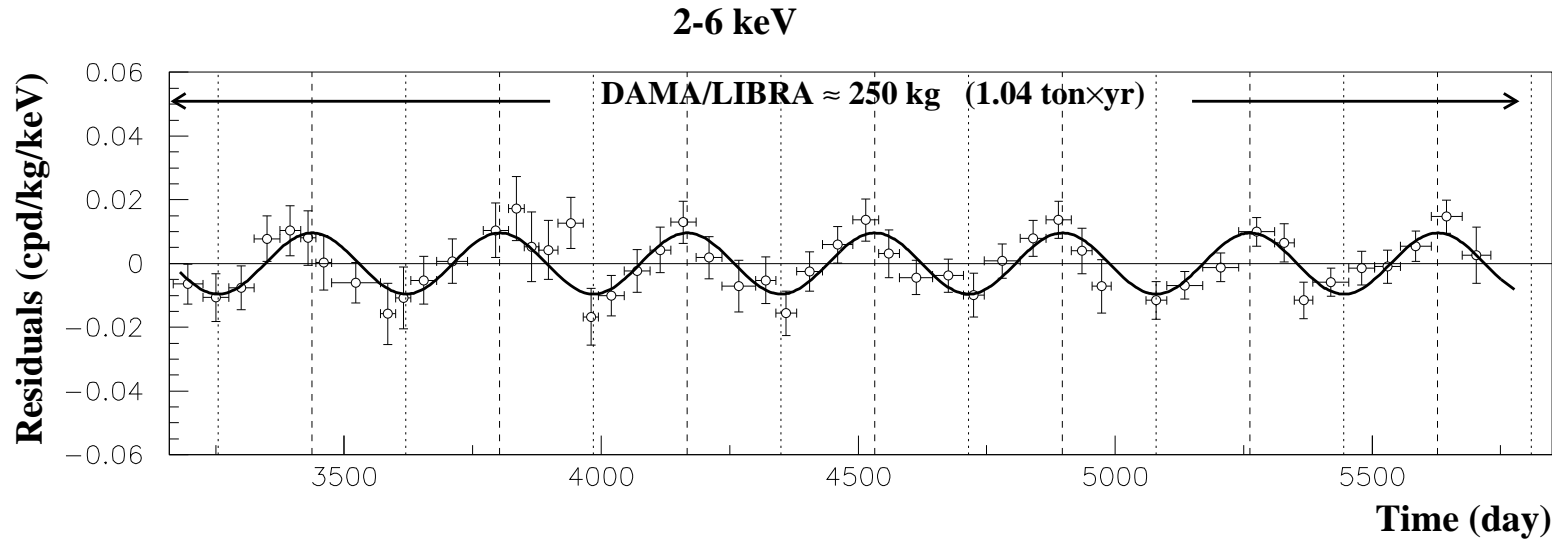
Direct Detection Technology Summary

Project	Strengths	Weaknesses
Cryogenic Ge detectors (CDMS, Edelweiss, CRESST)	Proven background rejection, experience	Expensive to build/test detectors
Threshold Detectors (COUPP, SIMPLE, PICASSO)	Ultimate EM rejection, inexpensive, easy to change target material	Alpha backgrounds, no energy spectrum, scaling to large mass?
Single-phase LAr, LXe (DEAP, Clean, XMASS)	Simple and reasonably inexpensive	Not clear if rejection good enough, E thresholds high
Dual-phase LAr (Darkside, WARP)	Excellent EM rejection and relatively inexpensive compared with Xe, Ge	^{39}Ar reduction needed, $\sim \times 10$ more target mass needed than Ge or Xe, E threshold high
Dual-phase LXe (Xenon, LUX)	Suitable target for both SI and SD, low E threshold possible	Poor intrinsic EM rejection, low E performance not understood
Low pressure TPCs (DMTPC, Drift)	Directional detection of WIMPs possible	Very hard to get sufficient target mass, backgrounds unknown
Scintillating Crystals (DAMA/LIBRA, KIMS)	Annual modulation with large target mass	No background rejection. Long-term stability crucial
Ionization Detectors (CoGeNT, DAMIC,...)	Very low E threshold and good E resolution	Background rejection difficult and small target masses

There may not be one clear winner; all experiments run into backgrounds!

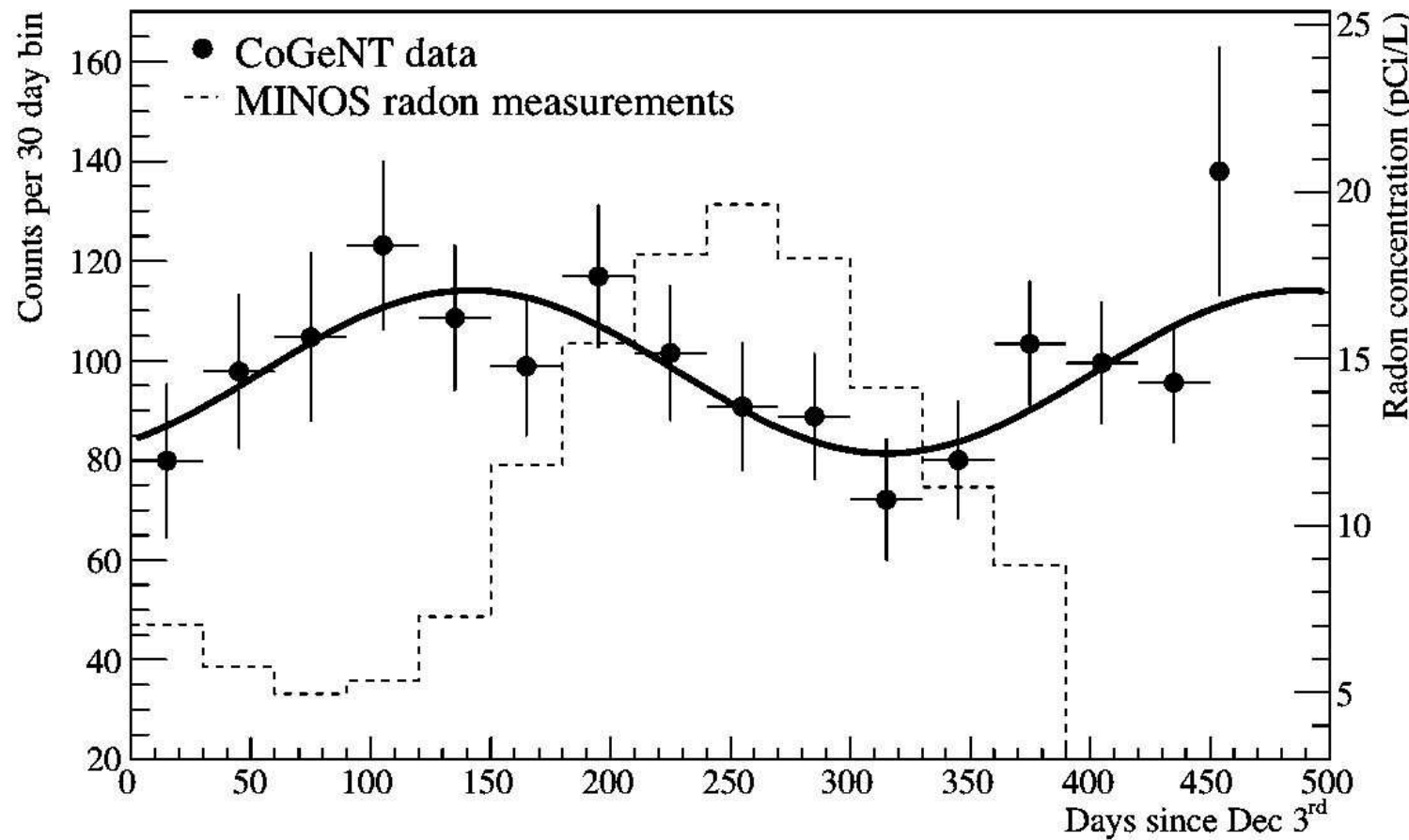
More than one technology will be needed to establish a WIMP signal

Annual modulation: Detection claim by DAMA/LIBRA Experiment



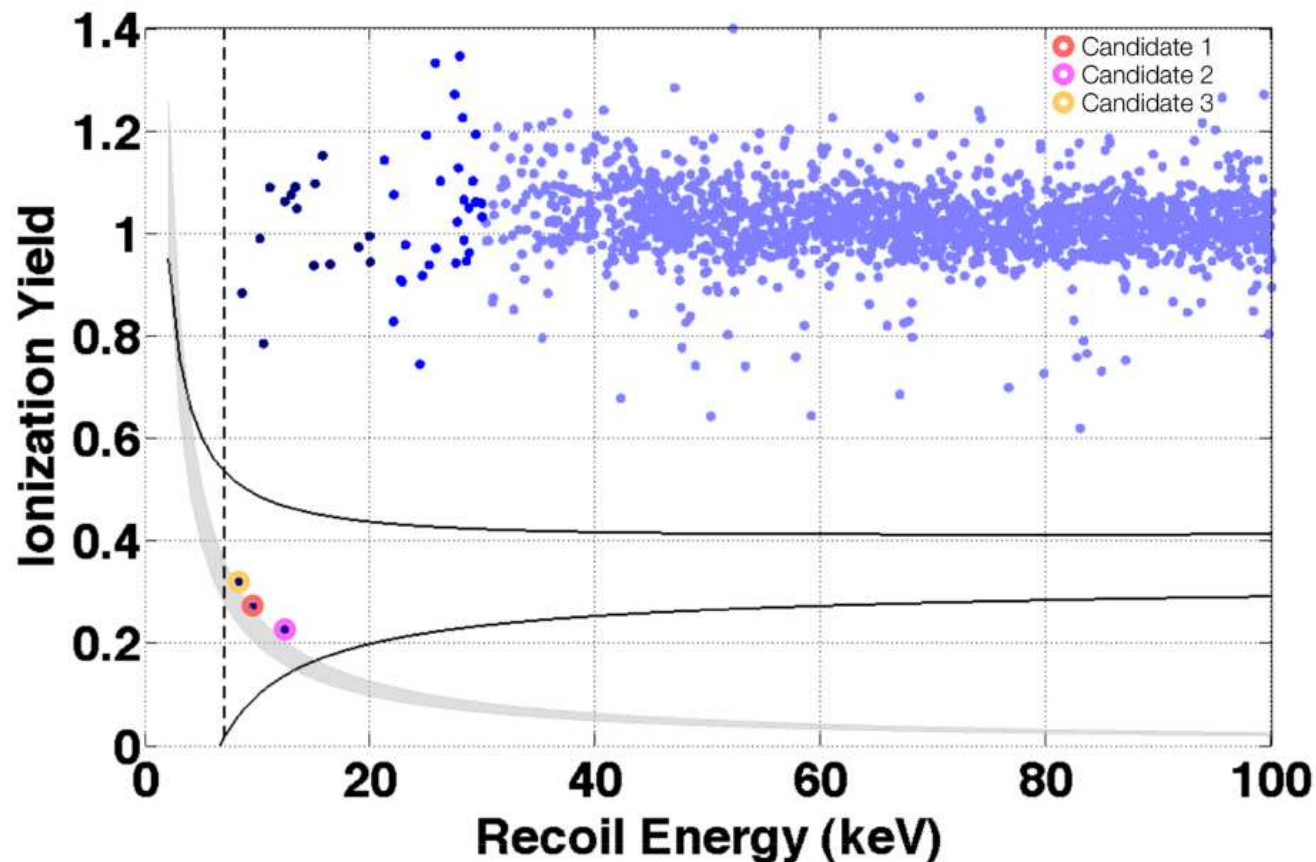
Temporal variation of single-hit event rate fitted with a sinusoidal curve: $A \cos \omega(t - t_0)$ with a period $T = \frac{2\pi}{\omega} = 1 \text{ yr}$, a phase $t_0 = 152.5 \text{ day}$ (June 2nd). The zero of the time scale is at January 1st of the first year of data taking of the former DAMA/NaI experiment. Dashed vertical lines: expected maximum (June 2nd). Dotted vertical lines: minimum. (Bernabei et al, arXiv:1308.5109)

Annual modulation in CoGeNT experiment



(Aalseth et al, arXiv:1208.5737

Direct Detection: CDMS Limits

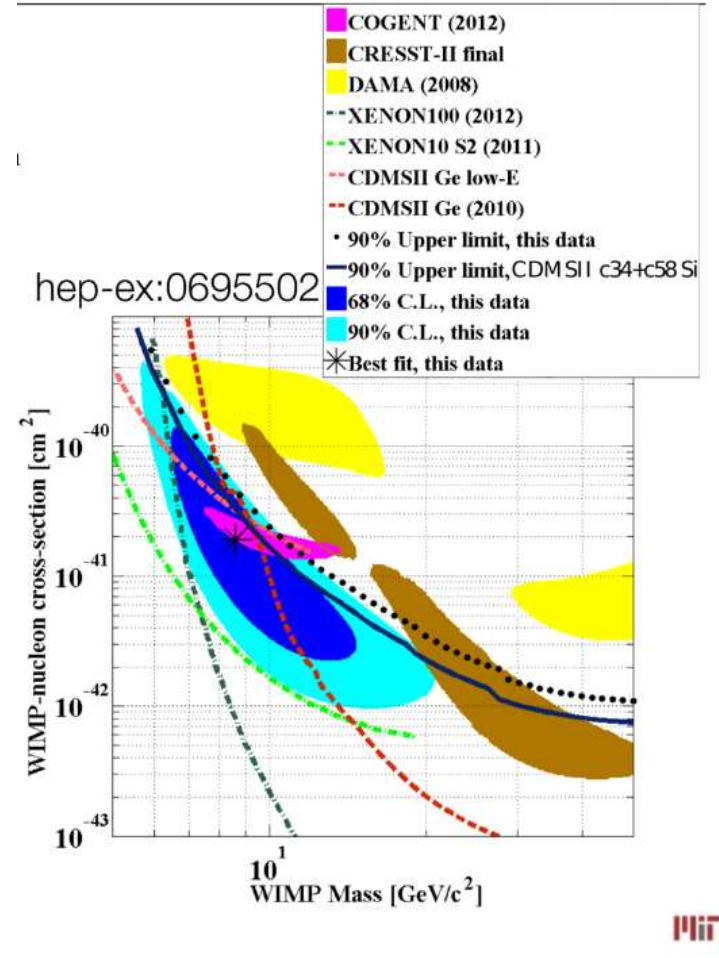


Kevin A. McCarthy / APS April Meeting / 2013



140.2 kg. day of Si data (July 2007 – Sept 2008): 3 low-mass (~ 8.6 GeV) WIMP candidate events!

Exclusion Plot



From Kevin McCarthy, APS meeting, April'13

But ... new results from Large Underground Xenon (LUX) detector

First results from the LUX dark matter experiment at the Sanford Underground Research Facility

D.S. Akerib,² H.M. Araújo,⁴ X. Bai,⁸ A.J. Bailey,⁴ J. Balajthy,¹⁶ S. Bedikian,¹⁹ E. Bernard,¹⁹ A. Bernstein,⁶ A. Bolozdynya,² A. Bradley,² D. Byram,¹⁸ S.B. Cahn,¹⁹ M.C. Carmona-Benitez,^{2, 14} C. Chan,¹ J.J. Chapman,¹ A.A. Chiller,¹⁸ C. Chiller,¹⁸ K. Clark,² T. Coffey,² A. Currie,⁴ A. Curioni,¹⁹ S. Dazeley,⁶ L. de Viveiros,⁷ A. Dobi,¹⁶ J. Dobson,¹⁵ E.M. Dragowsky,² E. Druszkiewicz,¹⁷ B. Edwards,^{19, *} C.H. Faham,^{1, 5} S. Fiorucci,¹ C. Flores,¹³ R.J. Gaitskell,¹ V.M. Gehman,⁵ C. Ghag,¹¹ K.R. Gibson,² M.G.D. Gilchriese,⁵ C. Hall,¹⁶ M. Hanhardt,^{8, 9} S.A. Hertel,¹⁹ M. Horn,¹⁹ D.Q. Huang,¹ M. Ihm,¹² R.G. Jacobsen,¹² L. Kastens,¹⁹ K. Kazkaz,⁶ R. Knoche,¹⁶ S. Kyre,¹⁴ R. Lander,¹³ N.A. Larsen,¹⁹ C. Lee,² D.S. Leonard,¹⁶ K.T. Lesko,⁵ A. Lindote,⁷ M.I. Lopes,⁷ A. Lyashenko,¹⁹ D.C. Malling,¹ R. Mannino,¹⁰ D.N. McKinsey,¹⁹ D.-M. Mei,¹⁸ J. Mock,¹³ M. Moongweluwan,¹⁷ J. Morad,¹³ M. Morii,³ A.St.J. Murphy,¹⁵ C. Nehrkorn,¹⁴ H. Nelson,¹⁴ F. Neves,⁷ J.A. Nikkel,¹⁹ R.A. Ott,¹³ M. Pangilinan,¹ P.D. Parker,¹⁹ E.K. Pease,¹⁹ K. Pech,² P. Phelps,² L. Reichhart,¹¹ T. Shutt,² C. Silva,⁷ W. Skulski,¹⁷ C.J. Sofka,¹⁰ V.N. Solovov,⁷ P. Sorensen,⁶ T. Stiegler,¹⁰ K. O'Sullivan,¹⁹ T.J. Sumner,⁴ R. Svoboda,¹³ M. Sweany,¹³ M. Szydagis,¹³ D. Taylor,⁹ B. Tennyson,¹⁹ D.R. Tiedt,⁸ M. Tripathi,¹³ S. Uvarov,¹³ J.R. Verbus,¹ N. Walsh,¹³ R. Webb,¹⁰ J.T. White,^{10, †} D. White,¹⁴ M.S. Witherell,¹⁴ M. Wlasenko,³ F.L.H. Wolfs,¹⁷ M. Woods,¹³ and C. Zhang¹⁸

¹ Brown University, Dept. of Physics, 182 Hope St., Providence RI 02912, USA

² Case Western Reserve University, Dept. of Physics, 10900 Euclid Ave, Cleveland OH 44106, USA

³ Harvard University, Dept. of Physics, 17 Oxford St., Cambridge MA 02138, USA

⁴ Imperial College London, High Energy Physics, Blackett Laboratory, London SW7 2BZ, UK

⁵ Lawrence Berkeley National Laboratory, 1 Cyclotron Rd., Berkeley CA 94720, USA

⁶ Lawrence Livermore National Laboratory, 7000 East Ave., Livermore CA 94550, USA

⁷ LIP-Coimbra, Department of Physics, University of Coimbra, Rua Larga, 3004-516 Coimbra, Portugal

⁸ South Dakota School of Mines and Technology, 501 East St Joseph St., Rapid City SD 57701, USA

⁹ South Dakota Science and Technology Authority,

Sanford Underground Research Facility, Lead, SD 57754, USA

¹⁰ Texas A & M University, Dept. of Physics, College Station TX 77843, USA

¹¹ University College London, Department of Physics and Astronomy, Gower Street, London WC1E 6BT, UK

¹² University of California Berkeley, Department of Physics, Berkeley CA 94720, USA

¹³ University of California Davis, Dept. of Physics, One Shields Ave., Davis CA 95616, USA

¹⁴ University of California Santa Barbara, Dept. of Physics, Santa Barbara, CA, USA

¹⁵ University of Edinburgh, SUPA, School of Physics and Astronomy, Edinburgh, EH9 3JZ, UK

¹⁶ University of Maryland, Dept. of Physics, College Park MD 20742, USA

¹⁷ University of Rochester, Dept. of Physics and Astronomy, Rochester NY 14627, USA

¹⁸ University of South Dakota, Dept. of Physics, 414E Clark St., Vermillion SD 57069, USA

¹⁹ Yale University, Dept. of Physics, 217 Prospect St., New Haven CT 06511, USA

(Dated: October 30, 2013)

The Large Underground Xenon (LUX) experiment, a dual-phase xenon time-projection chamber operating at the Sanford Underground Research Facility (Lead, South Dakota), was cooled and filled in February 2013. We report results of the first WIMP search dataset, taken during the period April to August 2013, presenting the analysis of 85.3 live-days of data with a fiducial volume of 118 kg. A profile-likelihood analysis technique shows our data to be consistent with the background-only hypothesis, allowing 90% confidence limits to be set on spin-independent WIMP-nucleon elastic scattering with a minimum upper limit on the cross section of 7.6×10^{-46} cm² at a WIMP mass of 33 GeV/c². We find that the LUX data are in strong disagreement with low-mass WIMP signal interpretations of the results from several recent direct detection experiments.

LUX Exclusion Plot

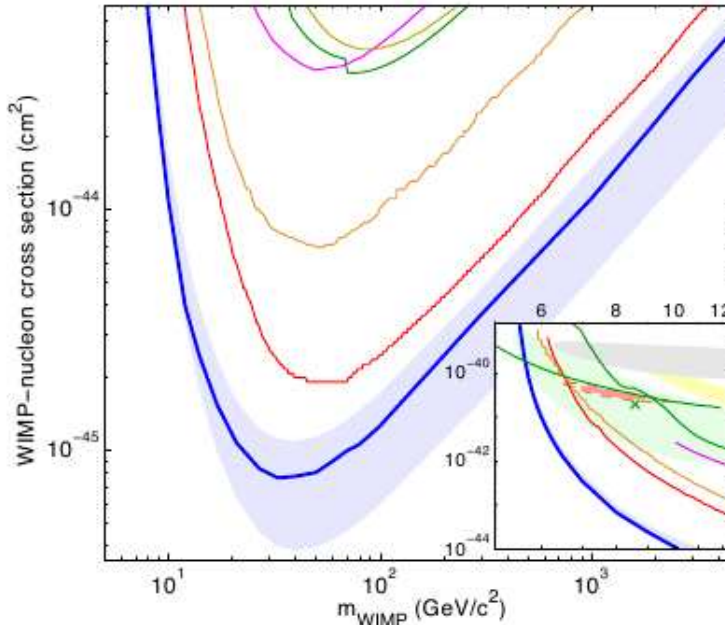
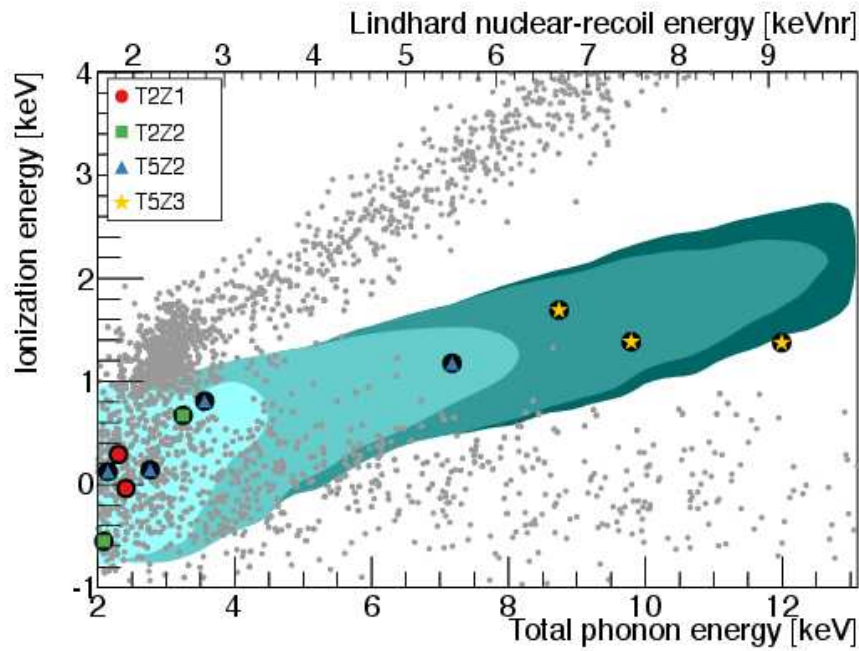


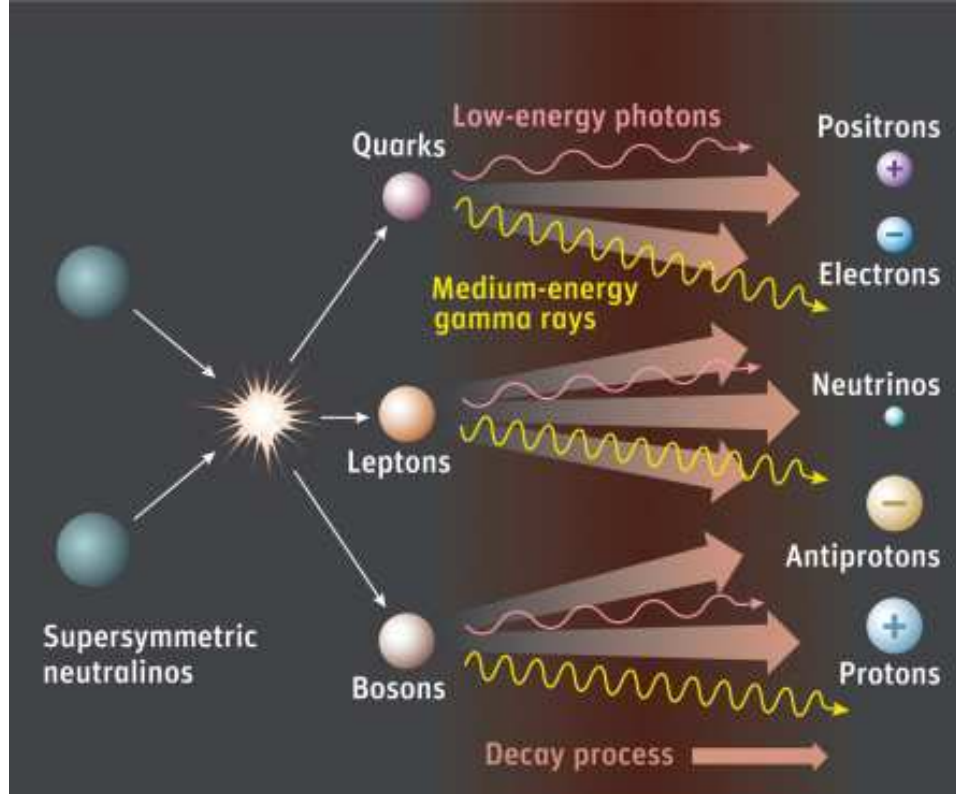
FIG. 5. The LUX 90% confidence limit on the spin-independent elastic WIMP-nucleon cross section (blue), together with the $\pm 1\sigma$ variation from repeated trials, where trials fluctuating below the expected number of events for zero BG are forced to 2.3 (blue shaded). We also show Edelweiss II [41] (dark yellow line), CDMS II [42] (green line), ZEPLIN-III [43] (magenta line) and XENON100 100 live-day [44] (orange line), and 225 live-day [45] (red line) results. The inset (same axis units) also shows the regions measured from annual modulation in CoGeNT [46] (light red, shaded), along with exclusion limits from low threshold re-analysis of CDMS II data [47] (upper green line), 95% allowed region from CDMS II silicon detectors [48] (green shaded) and centroid (green x), 90% allowed region from CRESST II [49] (yellow shaded) and DAMA/LIBRA allowed region [50] interpreted by [51] (grey shaded).

SuperCDMS results



$\sigma_{\chi-n}^{\text{SI}} < 1.2 \times 10^{-42} \text{ cm}^2$ at $m_\chi \sim 8 \text{ GeV}$ (But in tension with the results of LUX, CoGeNT, CDMS-Si, DAMA)

Indirect Detection: WIMP annihilation



AMS-2 positron excess, Fermi γ rays from dwSph, Galactic center, ...

Astrophysical issues

Expected number of events in direct detection (DD) or indirect detection (ID) experiments, and thus the interpretation of the results of these experiments, depend upon the density and velocity distribution of the WIMPs in the Galaxy.

$$\begin{array}{ccc} \text{No. of events (DD or ID)} & \equiv & \text{Particle Physics} \otimes \text{Astrophysics} \\ & & \downarrow \qquad \downarrow \\ & & (m_\chi, \sigma_{\chi N}) \otimes (\rho_{\text{DM}, \odot}, f(\mathbf{v})) \\ & & \downarrow \qquad \downarrow \\ & & \text{e.g., LHC} \otimes \text{Galactic Dynamics (e.g., rot. curve)} \end{array}$$

- Need to fix Astrophysics to extract particle physics of DM (m_χ, σ).
- Use the observed rotation curve data of the Galaxy to determine the phase space DF of DM particles, i.e., $\rho_{\text{DM}, \odot}, f(\mathbf{v})$.
- Galactic rotation curve near solar location is significantly influenced by visible matter.
- **Self-consistent approach:** Determine the DF of the DM particles by self-consistently including the effect of known visible matter (VM) such that together (DM+VM) they give a good fit to the observed rotation curve data.

Phase space distribution of collisionless systems

⇒ Phase space DF satisfies collisionless Boltzmann (Vlasov) equation (CBE),

$$\frac{df}{dt} \equiv \frac{\partial f}{\partial t} + \mathbf{v} \cdot \nabla f - \nabla \Phi \cdot \frac{\partial f}{\partial \mathbf{v}} = 0.$$

Jeans Theorem: *Any steady-state solution of the CBE depends on the phase-space coordinates only through integrals of motion in the galactic potential, and any function of the integrals yields a steady-state solution of the CBE.*

Simplest choice: $f(\mathbf{x}, \mathbf{v}) = f(E)$, with $E = \Phi + \frac{1}{2}v^2$.

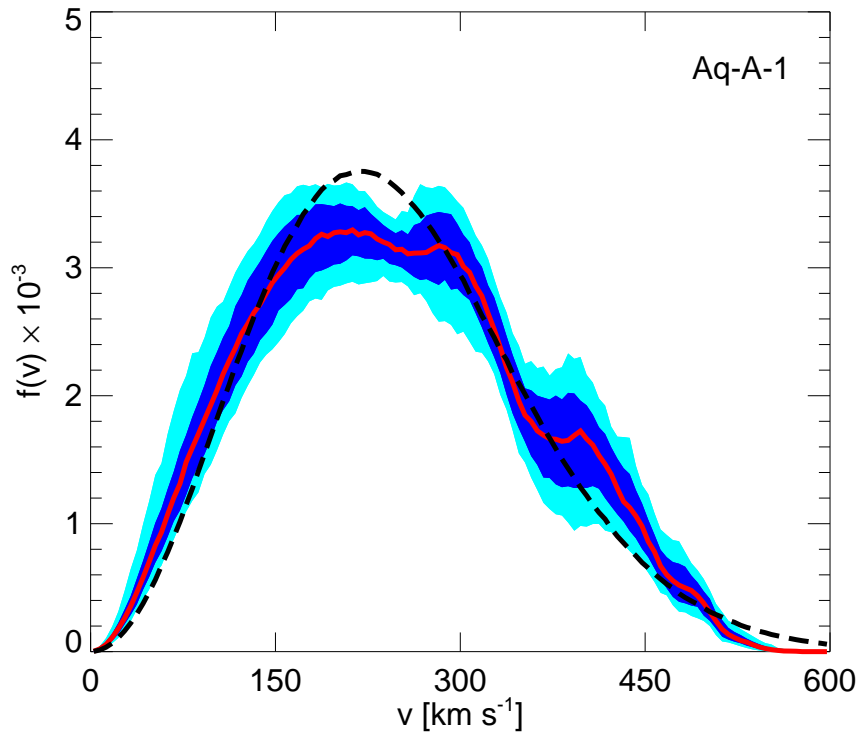
Isothermal DF:

$$f(\mathbf{x}, \mathbf{v}) = \frac{\rho_0}{(2\pi\sigma^2)^{\frac{3}{2}}} \exp[-E/\sigma^2],$$

with $\langle v^2 \rangle = 3\sigma^2$ and boundary condition $\Phi(0) = 0$, so that

$$\rho(\mathbf{x}) = \int f(\mathbf{x}, \mathbf{v}) d^3\mathbf{v} = \rho_0 \exp[-\Phi(\mathbf{x})/\sigma^2], \text{ and } \nabla^2 \Phi = 4\pi\rho_0 \exp[-\Phi(\mathbf{x})/\sigma^2].$$

DM Velocity Distribution: Simulations



(From Vogelsberger et al, arXiv:0812.0362)

The velocity distribution can be described by a “quasi-Maxwellian”.

The ‘Standard halo model’

Local WIMP velocity distribution, in the Galactic rest frame, is taken as **Maxwellian (isotropic isothermal sphere)**:

$$\begin{aligned} f^G(\mathbf{v}) &= N \left[\exp(-|\mathbf{v}|^2/v_c^2) - \exp(-v_{\text{esc}}^2/v_c^2) \right] & |\mathbf{v}| < v_{\text{esc}}, \\ f^G(\mathbf{v}) &= 0 & |\mathbf{v}| > v_{\text{esc}}, \end{aligned}$$

where N is a normalization factor, $v_c \approx 220 \text{ km s}^{-1}$ and $v_{\text{esc}} \approx (450 - 730) \text{ km s}^{-1}$ are the local circular and escape speeds respectively.

Usual fiducial value for the local WIMP density, $\rho_\chi = 0.3 \text{ GeV cm}^{-3}$.

For an **isothermal gravitating sphere**, $\langle v^2 \rangle^{1/2} = \sqrt{\frac{3}{2}} v_{c,\infty}$.

Assuming $v_{c,\infty} = v_{c,\odot} = 220 \text{ km s}^{-1}$, one has $\langle v^2 \rangle^{1/2} = 270 \text{ km s}^{-1}$.

Standard Halo Model (SHM) \equiv **Maxwellian** velocity distribution with

$\rho_{\text{DM},\odot} = 0.3 \text{ GeV/cm}^3$ and $\langle v^2 \rangle_{\text{DM},\odot}^{1/2} = 270 \text{ km s}^{-1}$.

Problems with SHM

- Isothermal sphere has $\rho \propto r^{-2}$ for large r . $\Rightarrow M(r) \rightarrow \infty$ as $r \rightarrow \infty$.
 \Rightarrow Need to truncate it, but must do so self-consistently, else not a solution of CBE.
- DF of DM at solar neighborhood is strongly influenced by visible matter. Need to self-consistently include the effects of visible matter to determine $\rho_{\text{DM}, \odot}$ and $f(v_{\text{DM}})_{\odot}$.

Two approaches:

- Make a reasonable ansatz for the DF of a finite gravitating system that is a solution of CBE, self-consistently include the effect of VM, and determine the parameters of the model so as to fit the rotation curve data of the Galaxy.

Or,

- Assume a parametrized form of the density profile of DM (based on, e.g., results of numerical simulations) in presence of the (known) VM, determine the parameters by a fit to the rotation curve data, and then ‘invert’ the density profile to derive the DF by Eddington’s (1916) method.

Truncated (“lowered”) Isothermal – “King model”

$$f(x, v) \equiv f(\varepsilon) = \begin{cases} \rho_1 (2\pi\sigma^2)^{-3/2} \left(e^{\varepsilon/\sigma^2} - 1 \right) & \text{for } \varepsilon > 0, \\ 0 & \text{for } \varepsilon \leq 0, \end{cases} \quad (1)$$

with

$$\varepsilon \equiv \Phi_0 - \left(\frac{1}{2}v^2 + \Phi \right), \text{ and } \Phi = \Phi_{\text{vis}} + \Phi_{\text{DM}} \equiv \Phi_{\text{total}}.$$

$$\nabla^2 \Phi_{\text{DM}}(R, z) = 4\pi G \rho_{\text{DM}}(R, z), \quad \nabla^2 \Phi_{\text{vis}}(R, z) = 4\pi G \rho_{\text{vis}}(R, z).$$

$\rho_{\text{DM}} \equiv \rho_{\text{DM}}[\Phi_{\text{vis}} + \Phi_{\text{DM}}] = \int f d^3v$. Note **Self-consistency**.

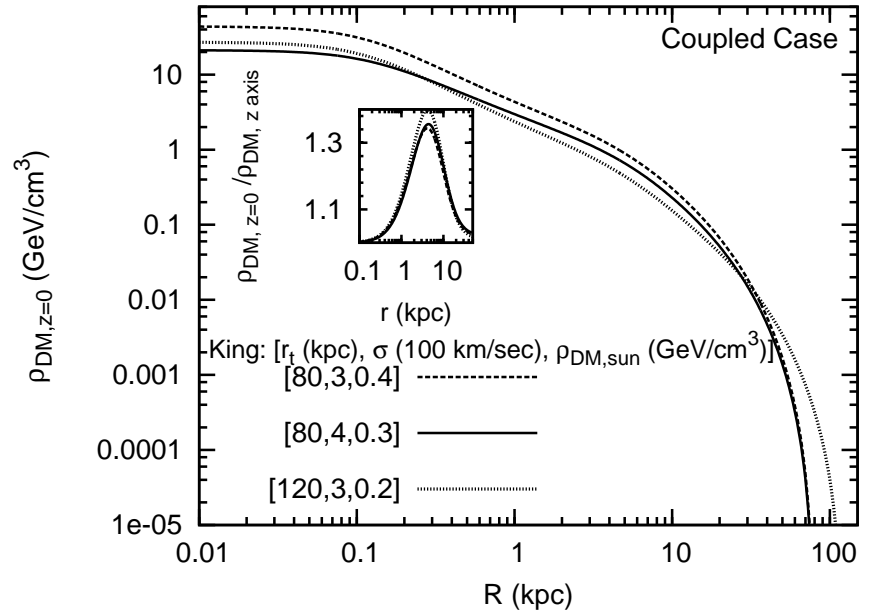
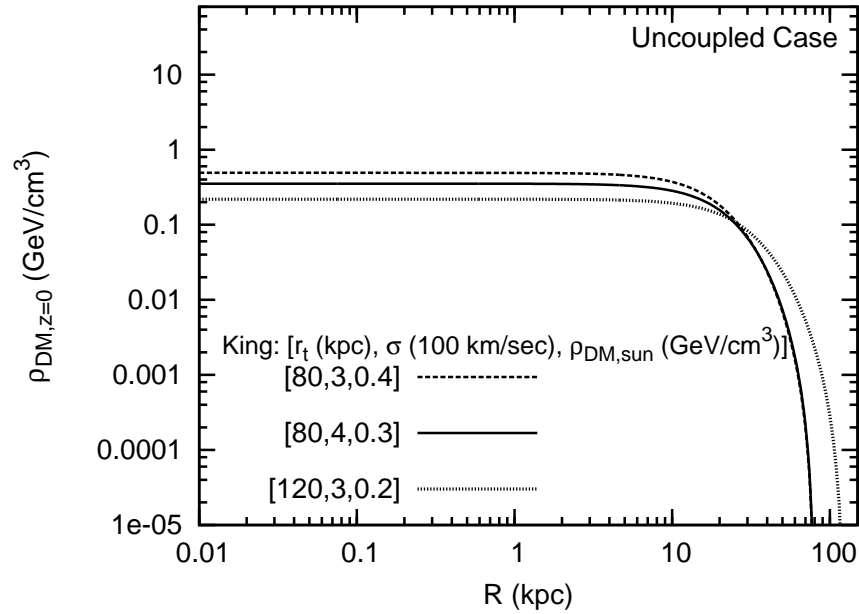
Three parameters: ρ_1 , σ and Φ_0 .

ρ_{DM} vanishes at $r = r_t$ where $\varepsilon = 0$.

Three “measurable” parameters of the model:

$$\rho_{\text{DM}, \odot} = \rho_{\text{DM}}(R = R_0, 0), \quad \langle v^2 \rangle_{\text{DM}, \odot}^{1/2} = \langle v^2 \rangle_{\text{DM}}^{1/2}(R = R_0, 0), \quad \text{and} \quad r_t.$$

Self-consistent DM Density Profile



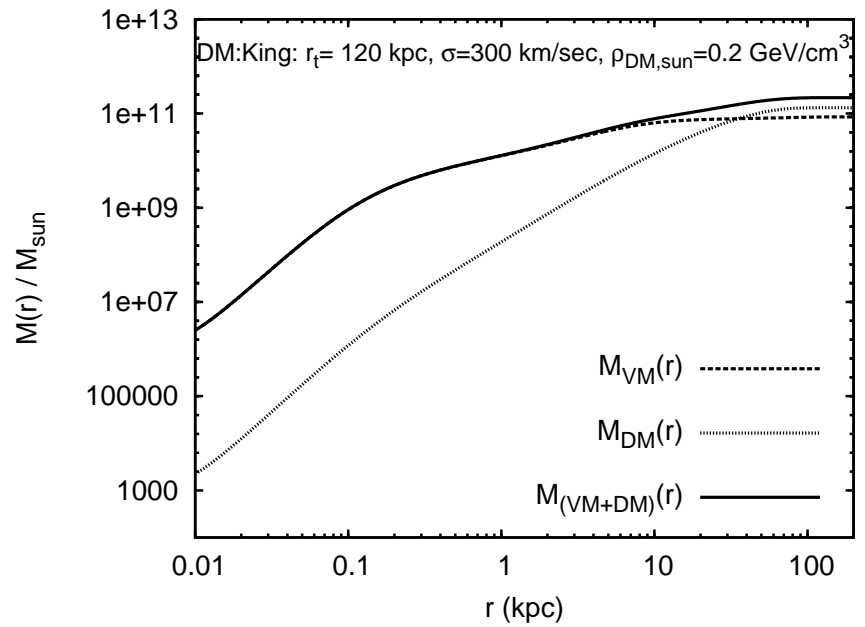
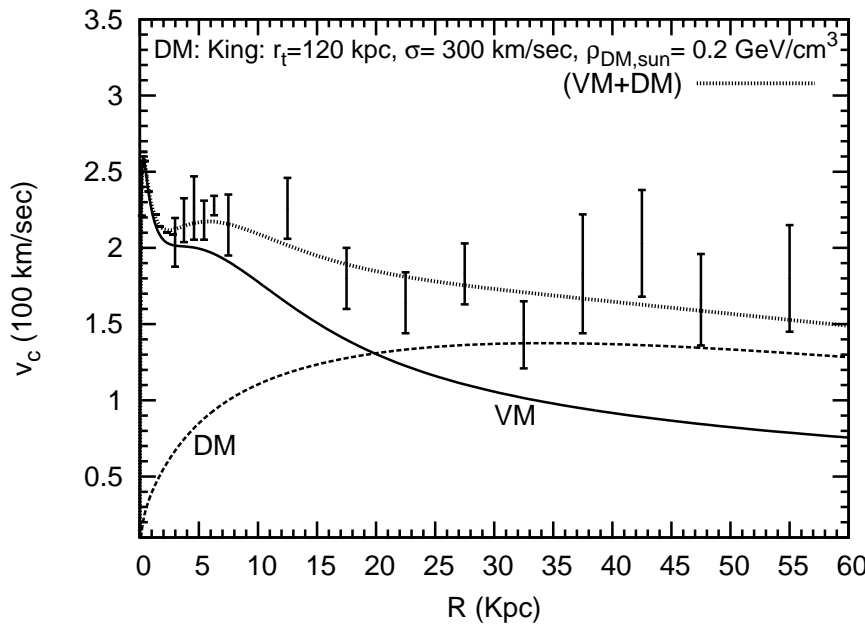
(S. Chaudhury, PB, R. Cowsik, JCAP (2010))

Visible matter “pulls in” the DM; DM density profile made steeper with enhanced density in the inner Galaxy

⇒ Impact on DM annihilation signals from the Galaxy Centre region

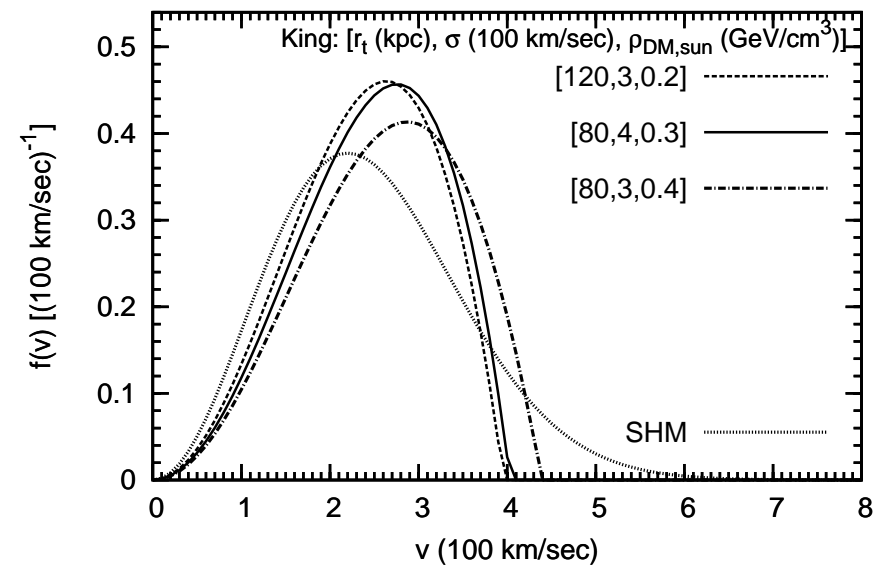
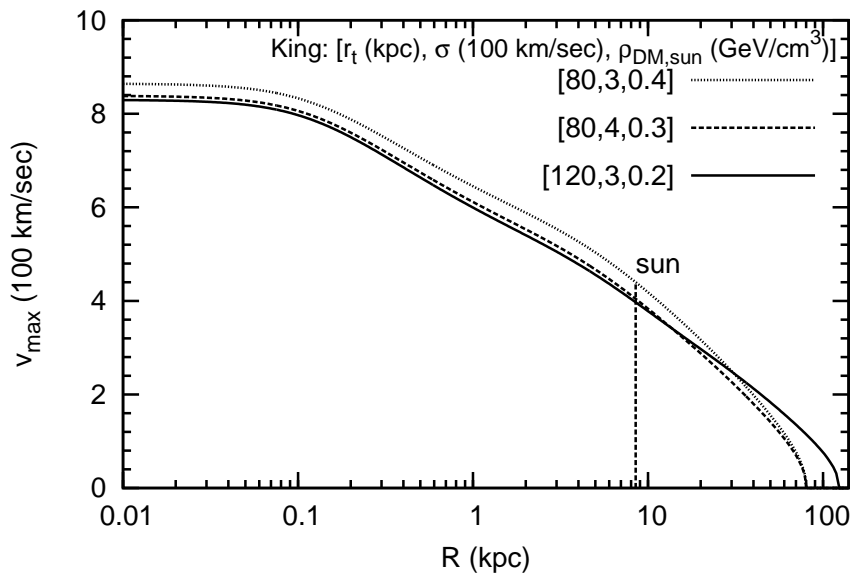
Rotation Curves for Truncated Isothermal Models

$$v_c^2(R) = R \frac{\partial \phi}{\partial R}(R, 0) = R \frac{\partial}{\partial R} [\phi_{\text{DM}}(R, 0) + \phi_{\text{vis}}(R, 0)] .$$



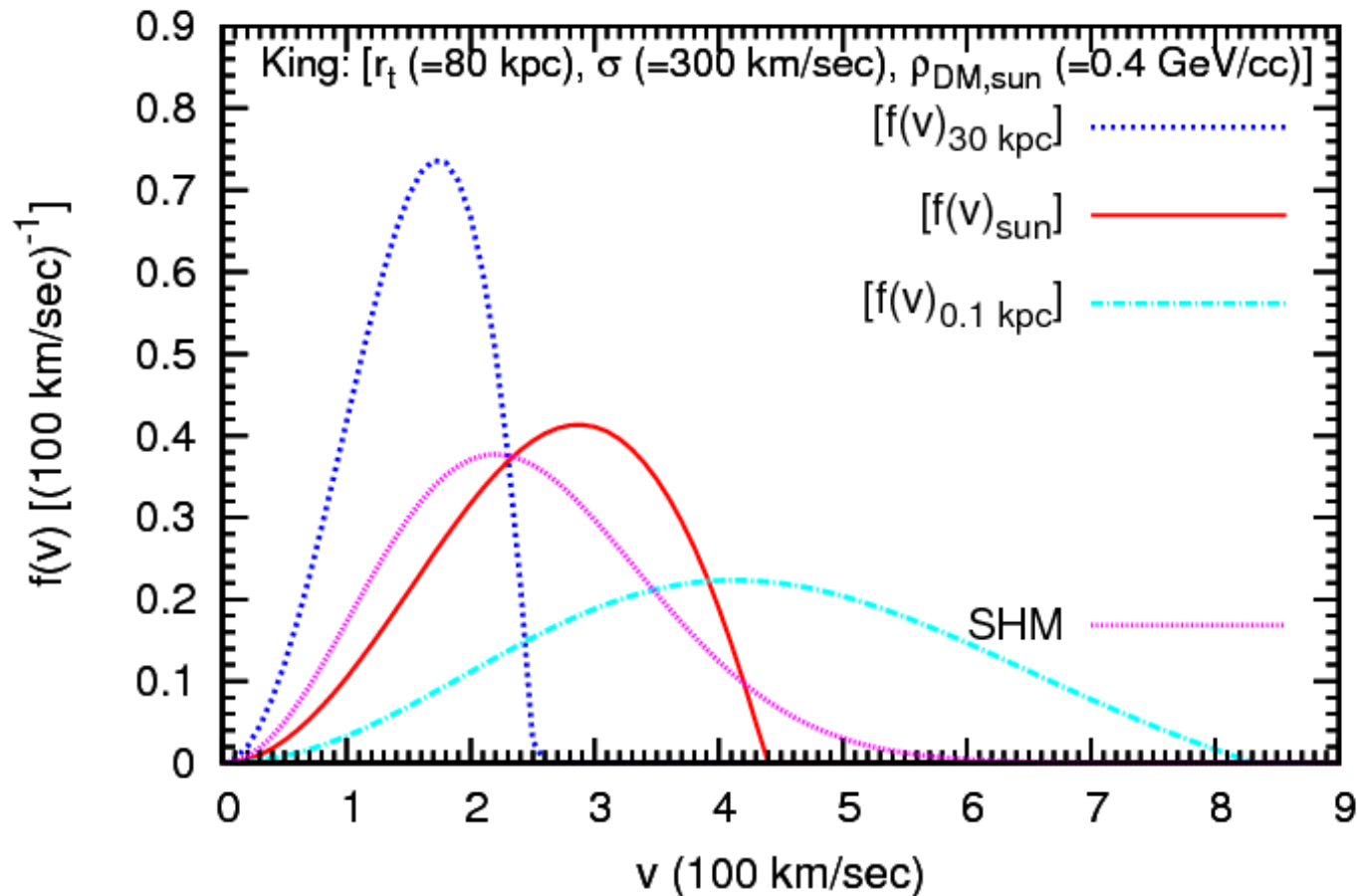
Rotation curve data out to 60 kpc (Xue et al (2008)) is used.

Self-consistent DM Velocity Distribution

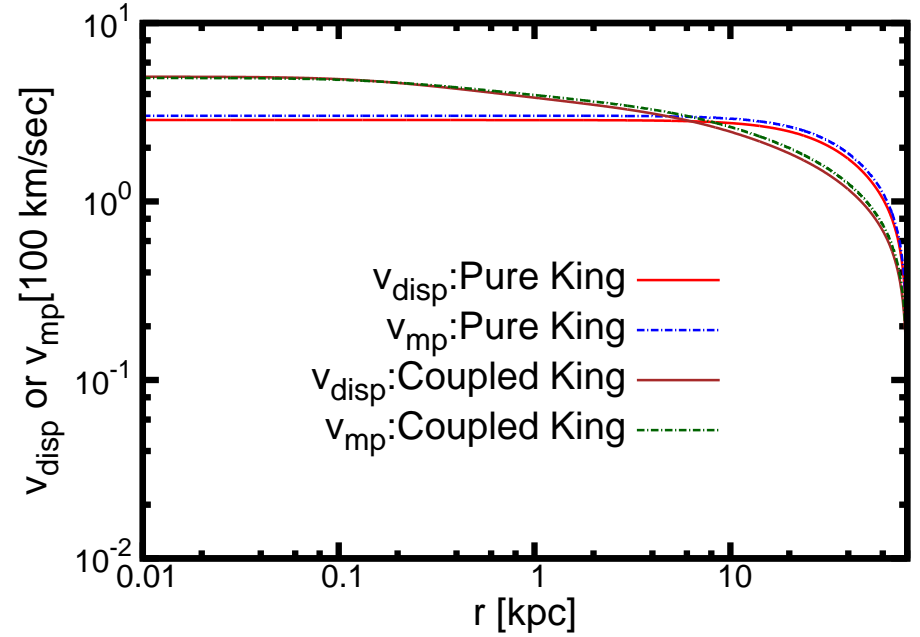
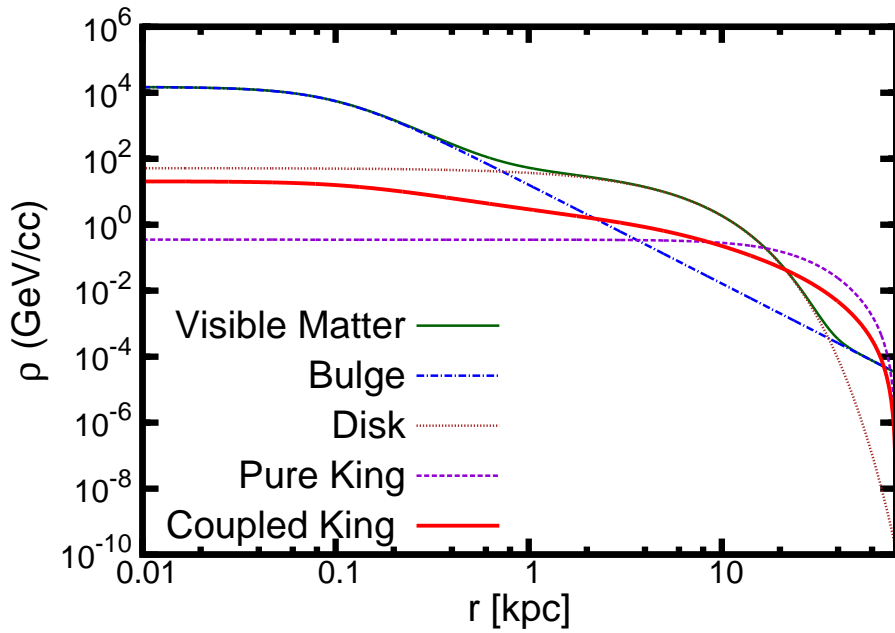


Non-Maxwellian velocity distribution; cutoff speed determined self-consistently

DM velocity distribution at various locations



DM density and velocity dispersion profiles



VDF from ρ : Eddington's Formula

For a given DF, $\mathcal{F}(\mathbf{x}, \mathbf{v})$, we get $\rho(\mathbf{x}) = \int d^3\mathbf{v} \mathcal{F}(\mathbf{x}, \mathbf{v})$.

Can we invert this? Given a $\rho(\mathbf{x})$ (or equivalently $\Phi(\mathbf{x})$), can we get a unique \mathcal{F} ?

Eddington (1916) : Possible for spherical systems with isotropic VDF, i.e., if $\mathcal{F}(\mathbf{x}, \mathbf{v}) \equiv \mathcal{F}(E)$, where $E = \frac{1}{2}v^2 + \Phi(r)$ = Total energy, i.e., if the system is "ergodic". Here $v = |\mathbf{v}|$, $r = |\mathbf{x}|$. Isotropic VDF $\Rightarrow \langle v_r^2 \rangle^{1/2} = \langle v_\theta^2 \rangle^{1/2} = \langle v_\phi^2 \rangle^{1/2}$. Eddington formula:

$$\mathcal{F}(\mathcal{E}) = \frac{1}{\sqrt{8\pi^2}} \left[\int_0^{\mathcal{E}} \frac{d\Psi}{\sqrt{\mathcal{E} - \Psi}} \frac{d^2\rho}{d\Psi^2} + \frac{1}{\sqrt{\mathcal{E}}} \left(\frac{d\rho}{d\Psi} \right)_{\Psi=0} \right],$$

where $\Psi(r) \equiv -\Phi(r) + \Phi(r = \infty)$ = relative potential and $\mathcal{E} \equiv -E + \Phi(r = \infty) = \Psi(r) - \frac{1}{2}v^2$ = relative energy.

Note, $\mathcal{F} > 0$ for $\mathcal{E} > 0$, and $\mathcal{F} = 0$ for $\mathcal{E} \leq 0$.

Also, $\rho(r) \Leftrightarrow \mathcal{F}(\mathcal{E})$ is unique iff $\int_0^{\mathcal{E}} \frac{d\Psi}{\sqrt{\mathcal{E}-\Psi}} \frac{d\rho}{d\Psi}$ is an increasing function of \mathcal{E} .

The VDF, $f_r(\mathbf{v}) = \mathcal{F}/\rho(r)$, has a natural truncation at $v(r) = v_{\max}(r) = \sqrt{2\Psi(r)}$.

Eddington inversion also possible for anisotropic VDF of certain special forms (Osipkov-Merrit)

VDF of DM particles by Eddington's Formula

$$\mathcal{F}(\mathcal{E}) = \frac{1}{\sqrt{8\pi^2}} \left[\int_0^{\mathcal{E}} \frac{d\Psi}{\sqrt{\mathcal{E} - \Psi}} \frac{d^2\rho}{d\Psi^2} + \frac{1}{\sqrt{\mathcal{E}}} \left(\frac{d\rho}{d\Psi} \right)_{\Psi=0} \right],$$

with $\Psi(r) \equiv -\Phi(r) + \Phi(r = \infty)$ and $\mathcal{E} = \Psi(r) - \frac{1}{2}v^2$.

We take $\rho(r) = \rho_{\text{DM}}(r)$. But note that $\Phi(r) \neq \Phi_{\text{DM}}(r)$.

Rather, $\Phi(r) = \Phi_{\text{DM}}(r) + \Phi_{\text{vis}}(r)$, since the DM particles “see” and move in the total gravitational potential including that of the visible matter. Actually, since visible matter is still the dominant component in the solar neighborhood. (DM dominates at larger distances), the VDF of DM in the inner regions of Galaxy is essentially determined by VM, not DM.

Parametrize Φ_{vis} and Φ_{DM} (or ρ_{DM}), and determine the parameters by MCMC fit to the observed rotation curve data, and then use Eddington formula to find $f_r(v)$ at any r .

Parametrize the densities:

$$\rho_{\text{vis}} = \rho_{\text{bulge}} + \rho_{\text{disk}}, \quad \nabla^2 \Phi_{\text{vis}}(R, z) = 4\pi G \rho_{\text{vis}}(R, z).$$

$$\rho_{\text{bulge}}(r) = \rho_{b0} \left(1 + (r/r_b)^2\right)^{-3/2},$$

$$\rho_{\text{disk}}(R, z) = \frac{\Sigma_{\odot}}{2z_d} \exp[-(R - R_0)/R_d] \exp[-|z|/z_d],$$

$$\rho_{\text{DM}}(r) = \rho_{\text{DM}, \odot} \left(\frac{R_0}{r}\right) \left(\frac{r_s + R_0}{r_s + r}\right)^2, \quad \nabla^2 \Phi_{\text{DM}}(R, z) = 4\pi G \rho_{\text{DM}}(R, z),$$

Rotation curve:

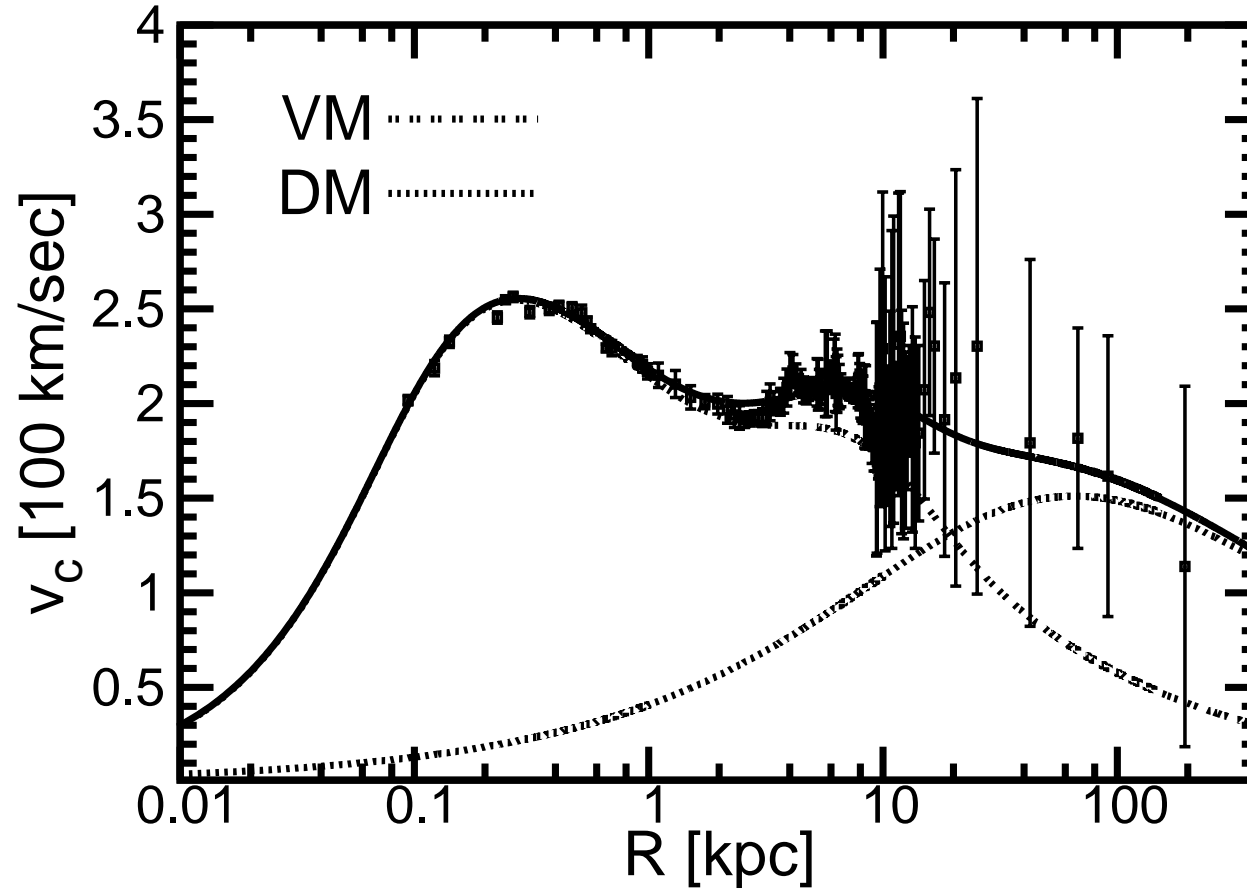
$$v_c^2(R) = R \frac{\partial}{\partial R} \left[\Phi_{\text{DM}}(R, z=0) + \Phi_{\text{vis}}(R, z=0) \right]$$

The seven parameters: r_s , $\rho_{\text{DM}, \odot}$, ρ_{b0} , r_b , Σ_{\odot} , z_d , and R_d , and their uncertainties are determined by MCMC fit to rotation curve data.

Eddington formula works for spherical systems. But disk is axisymmetric.

\Rightarrow Spherical approximation: $\Phi_{\text{vis}}(r) \simeq \int_0^r \frac{GM_{\text{vis}}(r')}{r'^2} dr'$ (error < 10%)

Fit to Rotation Curve



Rotation curve with best-fit values of DM and VM parameters. Data are from Y. Sofue, PASJ **64** (2012) 75; arXiv:1110.4431.

(PB, S.Chaudhury, S. Kundu, S. Majumdar, PRD (2013))

Dark Matter parameters

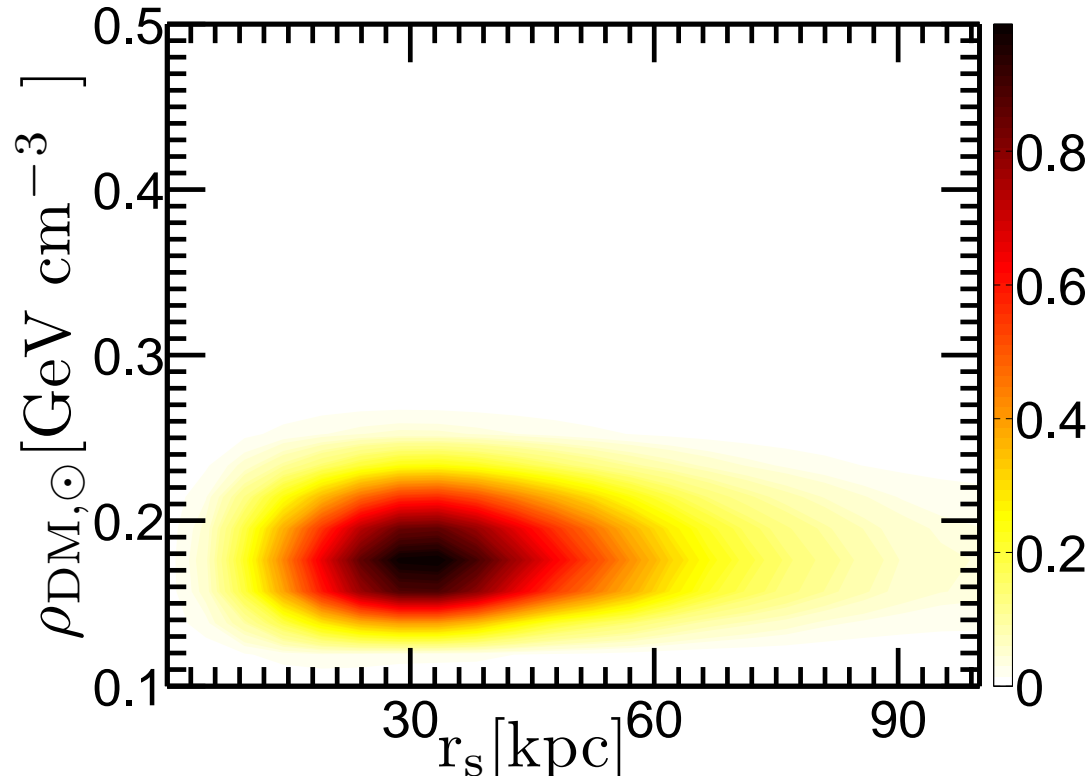


Figure 1: The 2D posterior probability density function for Dark Matter parameters ($r_s - \rho_{\text{DM}, \odot}$), marginalized over the visible matter parameters.

(PB, S.Chaudhury, S. Kundu, S. Majumdar, PRD (2013))

Dark Matter VDF

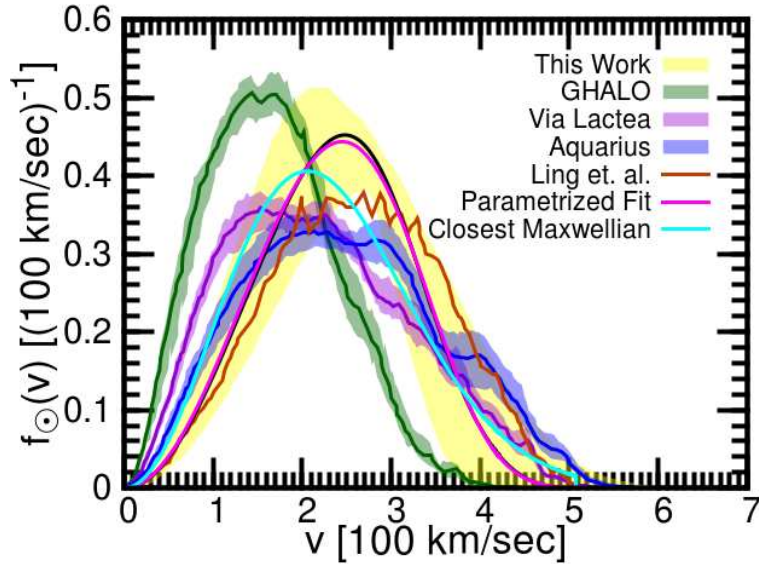


Figure 2: Normalized local speed distribution, $f_{\odot}(v)$, corresponding to the most-likely set of values of the Galactic model parameters determined from fit to rotation curve data, and its uncertainty band (shaded) corresponding to the 68% C.L. upper and lower ranges of the Galactic model parameters.

Best-fit (non-Maxwellian) speed distribution: $f_{\odot}(v) \approx 4\pi v^2 (\xi(\beta) - \xi(\beta_{\max}))$, where

$\xi(x) = (1+x)^k e^{-x^{(1-k)}}$, $\beta = v^2/v_0^2$, $\beta_{\max} = v_{\max,\odot}^2/v_0^2$, $v_0 = 339 \text{ km s}^{-1}$ and $k = -1.47$.

Impact on WIMP Direct Detection

Recoil spectrum: $\frac{d\mathcal{R}}{dE_R}(E_R, t) = \frac{\sigma(q^2=2m_N E_R)}{2m_\chi \mu^2} \rho_\chi g(E_R, t),$

with $\mu = m_\chi m_N / (m_\chi + m_N)$ = reduced mass, and

$$g(E_R, t) = \int_{u > u_{\min}(E_R)}^{u_{\max}(t)} \frac{d^3 \mathbf{u}}{u} f_\odot(\mathbf{u} + \mathbf{v}_E(t)) \Theta(u_{\max} - u_{\min}),$$

\mathbf{u} (with $u = |\mathbf{u}|$) = relative velocity of the WIMP with respect to the detector at rest on Earth

$\mathbf{v}_E(t)$ = time-dependent velocity of the Earth relative to the Galactic rest frame.

$u_{\min}(E_R) = (m_N E_R / 2\mu^2)^{1/2}$ = minimum WIMP speed required for producing a recoil energy E_R of the nucleus,

$u_{\max}(t)$ = lab frame (time-dependent) maximum WIMP speed corresponding to $v_{\max} = \sqrt{2\Psi}$ (defined in the Galactic rest frame).

Can show that $g(E_R, t)$ is a monotonically decreasing function of E_R , and thus takes its largest value at $E_R = E_{\text{th}}$.

The lowest WIMP mass that can be probed by a given experiment:

$$m_{\chi, \min} = m_N \left[\left(2m_N (v_{\max, \odot} + v_E)^2 / E_{\text{th}} \right)^{1/2} - 1 \right]^{-1}.$$

Define $\zeta \equiv g(E_R = E_{\text{th}})/g_{\text{Maxwell}}(E_R = E_{\text{th}})$

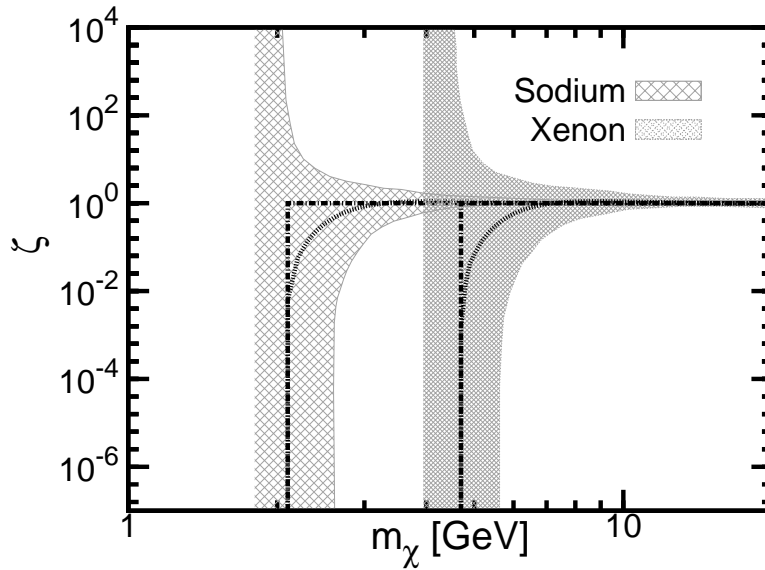


Figure 3: The ratio ζ for most-likely $f_{\odot}(v)$, with $E_{\text{th}} = 2 \text{ keV}$. The shaded bands correspond to the uncertainty bands of $f_{\odot}(v)$ from rotation curve. The calculations are for 2nd June, when the Earth's velocity in the Galactic rest frame is maximum.

Effect of departure from Maxwellian VDF is important for low m_{χ}

$\zeta \sim 10^{-2}$ at $m_{\chi} = m_{\chi, \text{min}}$!

Summarizing . . .

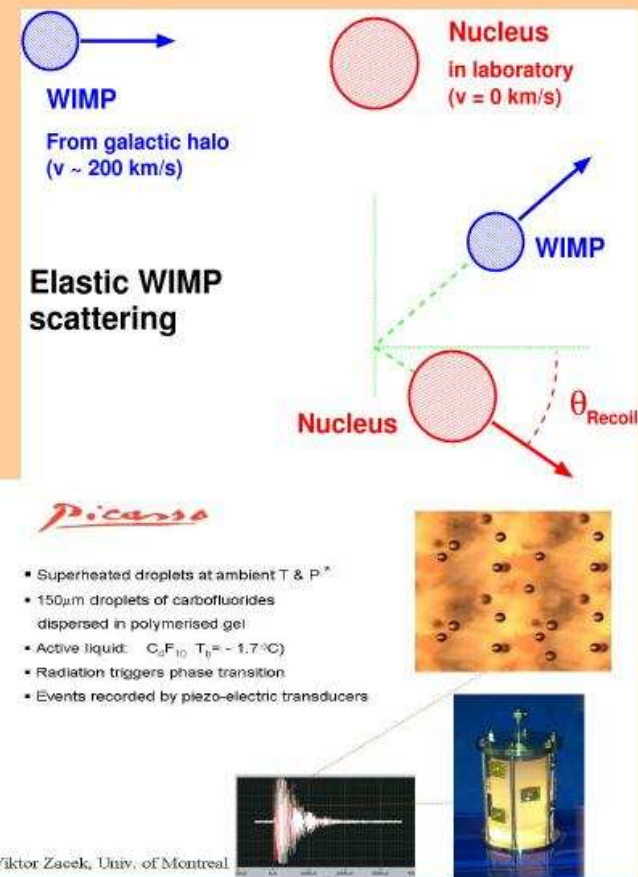
- WIMPs are natural candidates for the Dark Matter in the Universe.
- Direct Detection experiments have already achieved sensitivity at the level of $\sim 10^{-9}$ pb for SI WIMP-nucleus cross section. Some kinds of WIMPs may be close to detection, **if they are there!**
- Expected number of events in direct detection experiments depends on $\rho_{DM,\odot}$ and $f(v)_{DM,\odot}$. Must determine these parameters from observational data (e.g., Rotation Curve) by self-consistently including the gravitational effects of the visible matter.
- DM VDF is in general non-Maxwellian, and effect of departure from Maxwellian VDF is important for low-mass WIMPS — Maxwellian overestimates VDF at both high and low-velocity ends.
- Properly determined VDF will impact the interpretation of positron excess etc., from WIMP annihilation (Sommerfeld enhancement etc.).

Dark Matter search initiatives in India

PICASSO/PICO @ SNOLAB: Mainly sensitive to spin-dependent interactions

(mini)-DINO@ (Jaduguda)-INOLab: Mainly sensitive to spin-independent interactions

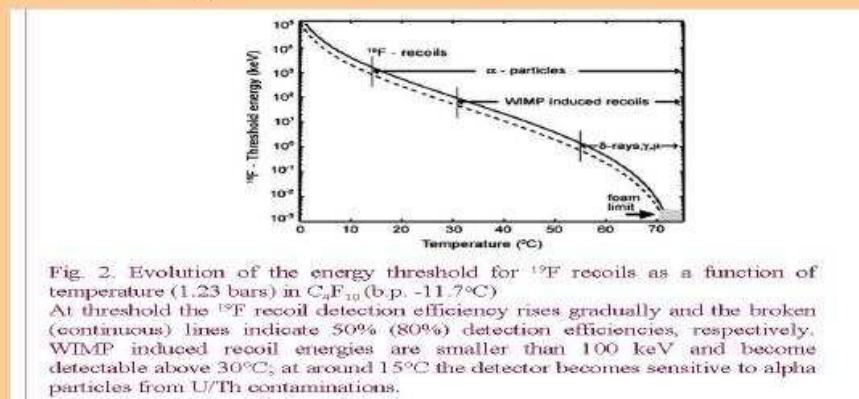
WIMP Dark Matter Search with Superheated Droplet Detector



Detect the recoiling nucleus with a Superheated Droplet Detector

A superheated liquid drop can vaporize due to energy deposited by the passage of the recoiling nucleus.

Vapour bubbles larger than a critical size expand and finally burst sending out acoustic waves through the medium (gel) in which the liquid drops are suspended. This acoustic signal can be picked up by suitable electronic sensors.



Barnabe-Heider et al *Phys. Lett. B* 624 (2005) 186

The PICASSO Collaboration

CANADA



USA



Czech Republic



INDIA



University of Alberta, Laurentian University, Universite de Montreal, Queen's University,
SNOLab, Bubble Technology Industries, CANADA

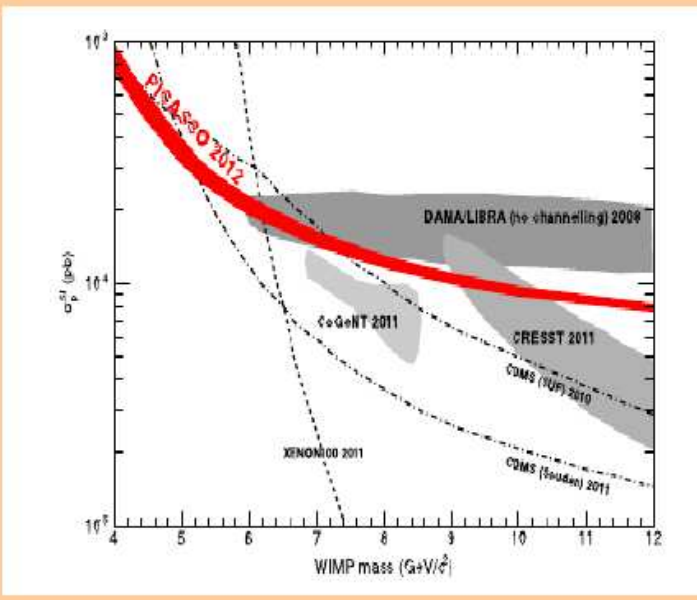
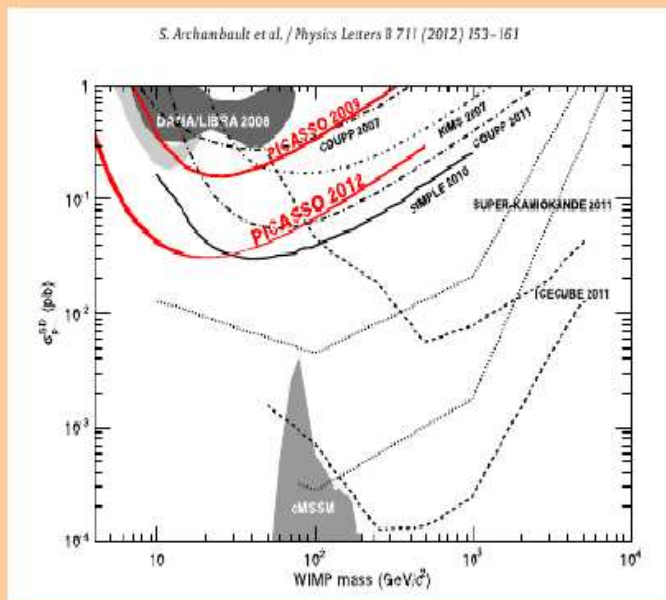
Indian University, Southbend, USA, Czech Technical University in Prague,
CAPP, Saha Institute of Nuclear Physics, INDIA

9 organizations from 4 countries with 28 people (at present)



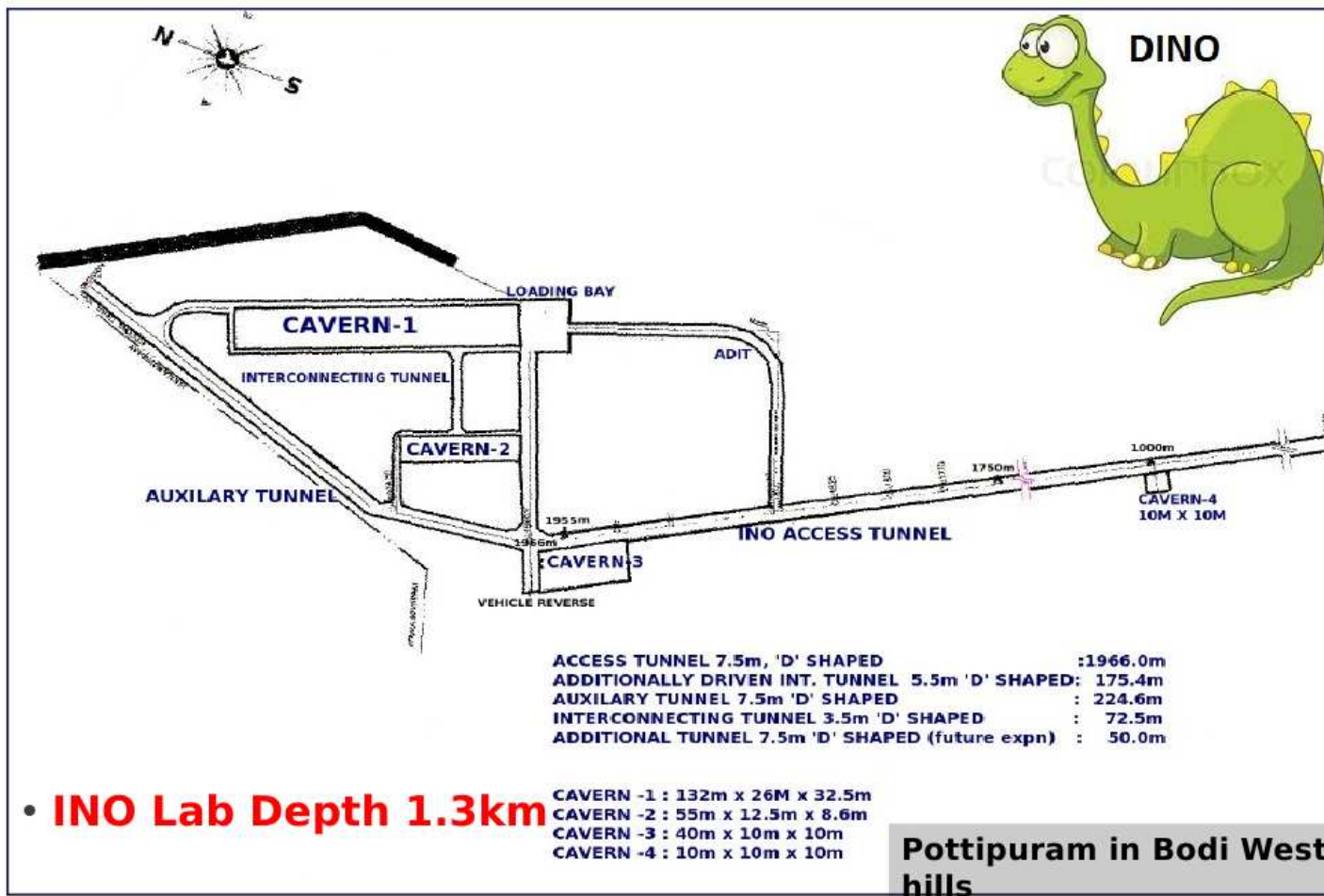
May 2009

PICASSO Results



Physics Letters B 711 (2012) 153

Dark-matter@INO (DINO) Ton-scale 2020



Mini-DINO @ UCIL-Jaduguda Mines

- A 15-30 kg Si/Ge detector for low-mass ($\lesssim 10$ GeV) WIMPs
- Two possibilities being explored:
 - (i) Use only ionization signal — can operate at 77 K or 4 K with few keV threshold.
No phonon sensors (which would require TES operating at mK temperatures).
 - (ii) Use both ionization and phonon signals at sub-keV threshold
- New iZIP detector technology developed at TAMU: can pick up low-ionization events due to nuclear recoils.
- Discrimination against high-ionization events due to electron recoils possible by pulse-shape-based analysis (R&D going on at SINP & TAMU)

Multi-institutional collaborative effort:

SINP (Kolkata), Texas A&M (TAMU, USA), NISER (Bhubaneswar), TIFR, IoP-Bhubaneswar,
PRL-Ahmedabad, . . .

With several DD and ID experiments running + LHC, the Dark Side of the Universe is looking bright indeed!

Acknowledgments :

Astrophysics & Direct/Indirect detection phenomenology:

Soumini Chaudhury, Susmita Kundu, Ramanath Cowsik, Subhabrata Majumdar,

...

Direct detection experiments: PICASSO, DINO

Mala Das, Susnata Seth, Satyajit Saha, Rupak Mahapatra, R. Ranganathan, ...